Quasi-incompressible Cahn–Hilliard fluids and topological transitions

By J. Lowengrub[1] and L. Truskinovsky[2]

[1] *Department of Mathematics,*
[2] *Department of Aerospace Engineering and Mechanics,*
University of Minnesota, Minneapolis, MN 55455, USA

Received 6 January 1997; revised 19 August 1997; accepted 20 November 1997

One of the fundamental problems in simulating the motion of sharp interfaces between immiscible fluids is a description of the transition that occurs when the interfaces merge and reconnect. It is well known that classical methods involving sharp interfaces fail to describe this type of phenomena. Following some previous work in this area, we suggest a physically motivated regularization of the Euler equations which allows topological transitions to occur smoothly. In this model, the sharp interface is replaced by a narrow transition layer across which the fluids may mix. The model describes a flow of a binary mixture, and the internal structure of the interface is determined by both diffusion and motion. An advantage of our regularization is that it automatically yields a continuous description of surface tension, which can play an important role in topological transitions. An additional scalar field is introduced to describe the concentration of one of the fluid components and the resulting system of equations couples the Euler (or Navier–Stokes) and the Cahn–Hilliard equations. The model takes into account weak non-locality (dispersion) associated with an internal length scale and localized dissipation due to mixing. The non-locality introduces a dimensional surface energy; dissipation is added to handle the loss of regularity of solutions to the sharp interface equations and to provide a mechanism for topological changes. In particular, we study a non-trivial limit when both components are incompressible, the pressure is kinematic but the velocity field is non-solenoidal (quasi-incompressibility). To demonstrate the effects of quasi-incompressibility, we analyse the linear stage of spinodal decomposition in one dimension. We show that when the densities of the fluids are not perfectly matched, the evolution of the concentration field causes fluid motion even if the fluids are inviscid. In the limit of infinitely thin and well-separated interfacial layers, an appropriately scaled quasi-incompressible Euler–Cahn–Hilliard system converges to the classical sharp interface model. In order to investigate the behaviour of the model outside the range of parameters where the sharp interface approximation is sufficient, we consider a simple example of a change of topology and show that the model permits the transition to occur without an associated singularity.

Keywords: immiscible binary fluids; numerical front capturing; level set methods; mixture theory; singularities on interfaces; variational methods

1. Introduction

In classical hydrodynamics, a narrow zone separating two ideal immiscible fluids is often represented as a discontinuity of density and tangential velocity. This is a good

Proc. R. Soc. Lond. A (1998) **454**, 2617–2654

approximation if the interfacial thickness is small compared with other characteristic scales of the flow. The classical fluid equations are then posed on both sides of the interface and jump conditions are prescribed across the surface of discontinuity. The sharp interface model, however, breaks down when the interfacial thickness becomes comparable to either the radius of curvature or the distance between surfaces. This happens, for example, when material surfaces collide. In this case, the collapse of the sharp interface model, which can be strongly enhanced by surface tension, is accompanied by topological singularities (see, for instance, Hou *et al*. 1994, 1997). Changes in interface topology are commonly observed in real fluid flows, with the standard example being the pinching and fissioning of liquid jets.

In this paper, following some previous work outlined below, we suggest a physically motivated regularization of the Euler equations which allows topological transitions to occur smoothly. In this model, the sharp interface is replaced by a narrow transition layer across which the fluids may mix. Although viscosity is known to be an important factor in topological transitions, it does not provide a regularization mechanism to transit through a topology change. An alternative mechanism of dissipation, which we explore in this paper as a regularization of the Euler equations, is the molecular mixing of 'immiscible' fluids in the thin transition layer. Our approach is motivated in part by the formal (computational) smoothing of flow discontinuities in the so-called level set method (e.g. Osher & Sethian 1988).

Traditionally, numerical simulations of sharp interface evolution have taken one of two forms: front tracking or front capturing. In the front tracking method, the position of the interface is explicitly traced, and, if necessary, the topology is changed by using an ad hoc rule (e.g. Mansour & Lundgren 1990; Univerdi & Trygvason 1992). In a few special cases, reconnection conditions can be derived directly from the Euler and Navier–Stokes equations by matching local similarity solutions valid near the transition point before and after pinch-off (e.g. Keller & Miksis 1983; Eggers & Dupont 1994; Eggers 1995).

In the front capturing method, an additional scalar field (level set function) is introduced whose zero level set marks the transition between the two fluid components. This method yields a singularity-free description of topological transitions and the internal structure of the interface layer is determined by explicit smoothing of the flow discontinuities. In spite of the general computational success of this method, which can be modified to include surface tension (Brackbill *et al*. 1994; Chang *et al*. 1996), one discovers that solutions depend essentially on the type of smoothing and, unless the fine structure of the interface is constantly modified, the level set function typically develops singularities in finite time (Sussman *et al*. 1994). This makes it natural to consider a physically realistic scalar field instead of an artificial level set function.

We suggest the mass concentration of one of the constituents as the additional field. This accounts for mixing (at the molecular level) in the interface region, a reflection of the partial miscibility that real fluids always display. According to the thermodynamics of 'immiscible' fluids, there is a range of concentrations where the free energy is concave and homogeneous states are unstable (e.g. Landau & Lifshitz 1958). An interface between two immiscible fluids can then be described as a layer where thermodynamically unstable mixtures are stabilized by weakly non-local (gradient) terms in the energy, an idea which can be traced to van der Waals (1894). This approach was first constructively used by Cahn & Hilliard (1958) in the context of a purely diffusional problem. In its original form, the Cahn–Hilliard (CH) model oversimplifies the physical situation by assuming that there is no coupling between diffusion and mechanics; in this setting, the model describes solids and fluids equally well. The coupling of the equations of fluid dynamics with CH diffusion is non-trivial because of the dependence of the energy upon concentration gradients and the associated reactive forces exerted on the fluid.

In this paper, following Truskinovsky (1993), we develop a thermodynamically and mechanically consistent model which extends the Euler (E) and Navier–Stokes (NS) models to the case of compressible binary CH mixtures. Compared to the classical equations of fluid mechanics, our system of equations includes two additional small parameters.

One parameter introduces an internal length scale (dispersion, non-locality) which yields extra non-hydrostatic (reactive) stresses even in the absence of viscosity. This gives rise to the effects of surface tension and provides an extra coupling between the fluid flow and the diffusion of the component. As a result, the fluid inside the transition layers behaves like an anisotropic solid. However, this solid is very special since the equations (in the dissipation free case) are compatible with a hydrodynamic Cauchy–Lagrange integral as well as with a Clebsch representation for the velocity field.

The other parameter prescribes the rate of non-viscous dissipation which is added to handle the loss of regularity of the solutions of the sharp interface model and to provide a mechanism for topological changes. Notice that the sharp interface model, which we consider as a limiting case, is dissipation free. Dissipation, therefore, becomes important where the sharp interface system breaks down, in particular, near the point of a topological transition. In this sense, topological transitions are similar to classical shock waves in hyperbolic conservation laws where the dissipation (usually due to viscosity) is relevant only inside the shock wave. This analogy is illuminating since shock waves generically occur in the level set model when the level set function is advected by a given velocity field (Sethian 1996). Our approach can then be interpreted as smoothing these shock waves by a diffusional, rather than a viscous, regularization.

This model fits naturally into the general framework of the so-called phase field models which have been widely used in the study of free boundary problems (see Gurtin & McFadden (1992) for a collection of recent references).

An abstract model which couples fluid flow with dissipative Ginzburg–Landau dynamics of a non-conserved order parameter (known as model E in the nomenclature of Hohenberg & Halperin (1977)) was suggested as a means to simulate smooth topology changes in interfacial flows of incompressible fluids by Goodman (1993, personal communication). Here we take an alternative approach and consider an order parameter which is conserved (concentration). An abstract model, which couples fluid flow with Cahn–Hilliard diffusion for a conserved order parameter, is known as model H (Hohenberg & Halperin 1977). Recently, Starovoitov (1994) and Gurtin *et al.* (1996) rederived model H by using the classical formalism of continuum mechanics. Jasnow & Vinals (1996) modified model H to study thermocapillary flow and gave an analysis of the Hamiltonian structure of the associated system of equations. Model H has been successfully used to simulate complicated mixing flows involving incompressible components with matched densities (see, for instance, Chella & Vinals 1996). This model, however, cannot be used if the incompressible fluid components have different densities (or if the fluids are compressible).

An important observation which distinguishes our model from model H is that binary fluids with incompressible components may in fact be compressible. We refer to such fluids as quasi-incompressible. In the non-trivial quasi-incompressible limit, the velocity field is non-solenoidal, even though the pressure is no longer defined by the thermodynamic formulas and is purely kinematic. Moreover, in this case, the chemical potential (which enters the diffusion equation) depends explicitly on the kinematic pressure.

The fact that the velocity field in quasi-incompressible mixtures can be non-solenoidal was recently pointed out by Joseph (1990) in the context of a theory describing the transient surface tension in mixtures of miscible fluids. His model, however, cannot be directly compared to ours since the transport of the component is based on the classical (local) diffusion equation, rather than the CH (non-local) model.

In the case of compressible fluids, considerable attention has been given to analysis of the van der Waals model (see, for instance, Davis & Scriven 1982) in which the energy depends on density gradients (rather than concentration gradients). This model provides a continuous description of interfaces between different phases of the same fluid. Some of the issues discussed in the general framework of this model are: kinetics of phase boundaries (Slemrod 1983; Truskinovsky 1982); gravity and capillary waves (Anderson & McFadden 1997); wetting phenomena (Seppecher 1996; Jacqmin 1998); and nucleation (Dell'Isolla *et al*. 1998). In Joseph's study of miscible fluids (see Joseph & Rennardy 1993), the coupling of the concentration field with fluid flow was based on a general Korteweg-type (non-variational) dependence of extra stresses on density gradients and the assumption of ideal mixing (see also Aifantis & Serrin 1983; Falk 1992).

The effects of compressibility in models with an extra non-conserved order parameter were considered in Truskinovsky (1988), where a (compressible) generalization of the reactive stress tensor and chemical potential of model H were derived. Consistent thermomechanical models of Ginzburg–Landau-type (model E) were later used by Roshin & Truskinovsky (1989) and Myasnikov *et al*. (1990) for simulations of acoustic and shock waves in relaxing fluids.

The fully compressible model for the fluid flow coupled with the evolutionary equation for the conserved order parameter (Cahn–Hilliard diffusion) was suggested in Truskinovsky (1993) (see Appendix A). Later, Antanovskii (1995) presented a derivation of a quasi-incompressible version which has some common features with the model discussed in this paper, although the crucial dependence of the chemical potential on the kinematic fluid pressure was missing.

Our derivation of the governing equations for the quasi-incompressible case differs in several important ways from the general case of binary compressible mixtures. For example, in the quasi-incompressible limit, the structure of the independent fluxes and forces in the entropy inequality has to be modified, and the description in terms of the Helmholtz free energy ceases to be complete. To demonstrate the effects of quasi-incompressibility, we analyse the linear stage of spinodal decomposition in one dimension. In the original treatment of this problem (Cahn 1961), the evolution of the concentration field does not cause any fluid motion. Here, we show that when the densities of the fluids are not perfectly matched, the evolution of the concentration field induces fluid motion even if the fluids are inviscid (compare with Koga & Kawasaki (1991) and Gurtin *et al*. (1996), where an overdamped (viscous) approximation was considered).

We then introduce a scaling that allows one to obtain the classical sharp interface model (with a finite surface tension) as a limit of the dissipative quasi-incompressible Euler–Cahn–Hilliard (ECH) equations. The corresponding separation of scales is valid when the radius of curvature of the layers and their relative distance is small compared with their thickness. Since the sharp interface model is conservative, the dissipative terms disappear in this limit, which suggests that localized topological transitions may be associated with localized dissipation. This general observation is supported by the fully nonlinear computations on the pinching of two-dimensional fluid–fluid jets, which we report elsewhere (Lowengrub *et al.* 1998*a*, *b*). In that work, calculations were performed by using the quasi-incompressible ECH model and the smooth break-up of a periodic jet into a system of droplets was captured. The transition is marked by an abrupt decrease in the energy, and the dissipation is localized, both spatially and temporally, near the point of the topological transition.

In order to investigate the behaviour of the model outside the range of parameters where the sharp interface approximation is sufficient, we consider a quasi-static description of the simplest topological transition: the annihilation (nucleation) of a spherical droplet. When the radius of curvature is comparable to the thickness of the layer, the classical behaviour associated with the Laplace formula is no longer observed. We show that the ECH model permits the topological transition to occur without an associated singularity. Our results, which are in accordance with an analysis of the CH model (Cahn & Hilliard 1959), suggest that the radius of curvature of the diffuse droplets never decreases below a certain minimum value and that the effective surface tension is a non-trivial function of the droplet size. We remark that non-trivial curvature corrections to the 'constant' surface energy have also been studied by using first principles modelling based on particular intermolecular potentials (see, for instance, Keller & Merchant 1991); the corresponding asymptotic expansions, however, are only valid at small curvatures.

In § 2, we begin with a motivation of the partial miscibility regularization from the perspective of a level set method and introduce specific expressions for the extra stress tensor and extra energy density associated with the level set field. In § 3, we give a new derivation of the Navier–Stokes–Cahn–Hilliard (NSCH) system and analyse the special structure of the non-hydrostatic reactive stress tensor. We also non-dimensionalize the NSCH system and introduce four independent dimensionless constants of the model. In § 4, we discuss the concept of quasi-incompressibility and derive the limiting system of governing equations. We then investigate its implications by including the effects of fluid motion in the classical analysis of spinodal decomposition. In § 5, we show that when the internal length scale goes to zero, an appropriately scaled quasi-incompressible system converges to the classical sharp interface model. In § 6, we study the alternative case when the radius of curvature is comparable to the thickness of the layer and consider the annihilation (or nucleation) of a spherical droplet. Section 7 contains some concluding remarks.

2. Motivation

We begin by recalling the classical model of an inviscid one-component compressible fluid at a constant temperature. The motion of the fluid is governed by the Euler equations,

$$\dot{\rho} + \rho \operatorname{div} \boldsymbol{v} = 0, \tag{2.1}$$

$$\rho \dot{v} - \operatorname{div} \boldsymbol{P} = 0, \tag{2.2}$$

where $\boldsymbol{v}$ is the fluid velocity, ρ is the fluid density, $\boldsymbol{P} = -(\rho^2 \partial f/\partial \rho)\mathbf{1}$ is the spherical stress tensor, and $f(\rho)$ is the specific free energy. The notation $\dot{(\,)} = (\,)_t + \boldsymbol{v} \cdot \nabla(\,)$ is used to denote the convective time derivative.

In the case of two immiscible fluids, equations (2.1) and (2.2) are assumed to hold in the two fluid domains which are separated by a single smooth interface $\Sigma(t) = \{\boldsymbol{x} \mid \zeta(\boldsymbol{x}, t) = 0\}$ that travels with the flow, i.e.

$$\dot{\zeta} = 0. \tag{2.3}$$

Let fluid 1 be in the domain Ω_1, where $\dot{\zeta}(\boldsymbol{x}, t) > 0$ and fluid 2 be in the domain Ω_2, where $\zeta(\boldsymbol{x}, t) < 0$. We use the indices 1 and 2 to denote the fluid quantities in the corresponding domains. Further, let $H(\zeta)$ be the Heaviside function. Then $\chi(\boldsymbol{x}, t) = H(\zeta(\boldsymbol{x}, t))$ is the characteristic function of the domain Ω_1. Introduce the density and velocity as follows:

$$\rho = \rho_1 \chi + \rho_2 (1 - \chi), \qquad \boldsymbol{v} = \boldsymbol{v}_1 \chi + \boldsymbol{v}_2 (1 - \chi). \tag{2.4}$$

Taking surface energy into account, the free energy can be written as

$$\rho f = \rho_1 f_1(\rho_1) \chi + \rho_2 f_2(\rho_2)(1 - \chi) + \sigma \delta_{\Sigma}(\boldsymbol{x}, t), \tag{2.5}$$

where $\delta_{\Sigma}(\boldsymbol{x}, t) = |\nabla \zeta| \delta(\zeta)$ is the surface delta function, $\delta(\zeta)$ is the one-dimensional delta function, and σ is the surface energy per unit area, which is assumed to be constant. The corresponding stress tensor $\boldsymbol{P}$ includes singular (in-plane) components and is given by

$$\boldsymbol{P} = -[p_1(\rho_1)\chi + p_2(\rho_2)(1 - \chi)]\mathbf{1} + \sigma(\mathbf{1} - \boldsymbol{n} \otimes \boldsymbol{n}) \delta_{\Sigma}(\boldsymbol{x}, t), \tag{2.6}$$

where $p_{1,2} = (\rho^2 \partial f/\partial \rho)_{1,2}$ and

$$\boldsymbol{n}(\boldsymbol{x}, t) = \frac{\nabla \zeta}{|\nabla \zeta|} \tag{2.7}$$

is the normal to the interface $\Sigma(t)$.

In order to derive the corresponding jump conditions on $\Sigma(t)$, we substitute (2.4) into the governing equations (2.1)–(2.3) and separate the regular and singular parts of the result by using the following relations:

$$\nabla H = \boldsymbol{n} \delta_{\Sigma}, \quad H_t = -D \delta_{\Sigma}, \tag{2.8}$$

$$\operatorname{div}(\boldsymbol{n} \otimes \boldsymbol{n}) = -2\kappa \boldsymbol{n} + (\mathbf{1} - \boldsymbol{n} \otimes \boldsymbol{n}) \nabla \ln |\nabla \zeta|, \tag{2.9}$$

where $D = -\zeta_t / |\nabla \zeta|$ is the normal velocity of the surface and κ is the mean curvature, which is chosen to be positive if the surface is convex. Then, we obtain the classical jump conditions,

$$[[\rho(D - \boldsymbol{v} \cdot \boldsymbol{n})]] = 0, \tag{2.10}$$

$$[[\rho(D - \boldsymbol{v} \cdot \boldsymbol{n})(\boldsymbol{v} \cdot \boldsymbol{t})]] = 0, \tag{2.11}$$

$$[[\rho(D - \boldsymbol{v} \cdot \boldsymbol{n})\boldsymbol{v} + p\boldsymbol{n}]] = 2\sigma\kappa\boldsymbol{n}, \tag{2.12}$$

where $\boldsymbol{t}$ is either of the two independent vectors tangential to the surface of discontinuity ($\boldsymbol{t} \cdot \boldsymbol{n} = 0$), and $[[\;]] = (\,)_1 - (\,)_2$ denotes the jump of limiting values across the interface. Since the surface $\Sigma(t)$ is advected by the flow, $(\boldsymbol{v}\cdot\boldsymbol{n})_{1,2}=D$, (2.10) and (2.11) are satisfied automatically while (2.12) reduces to the classical Laplace formula,

$$[[p]] = 2\sigma\kappa. \tag{2.13}$$

Although the classical sharp interface theory adequately describes the motion of smooth interfaces, the model breaks down when interfaces intersect or the surface curvature diverges (e.g. Hou *et al.* 1994, 1997). To describe the evolution beyond these singular events, a continuous description of the surface layer is necessary. A straightforward way to obtain such a description is to smooth the characteristic function χ and to derive a desingularized system of equations. This approach is known as a level set method, since the interface is assumed to be the zero level set of the function ζ. Below, we briefly sketch our version of this approach which includes a continuous description of surface tension (see also Brackbill *et al.* 1994; Chang *et al.* 1996; Sussman *et al.* 1994). For a general background on level set methods, we refer the reader to Sethian (1996).

Introduce a one-parameter sequence of functions χ_ε, representing smooth approximations of the Heaviside function $H(\zeta)$. An additional constraint must be imposed on the sequence χ_ε, in order to fix the numerical value of surface tension. Let us assume that

$$\lim_{\varepsilon\to 0}\int_{-\infty}^{+\infty} \varepsilon\chi_\varepsilon'(\zeta)^2\,\mathrm{d}\zeta = \sigma. \tag{2.14}$$

Then $\varepsilon\chi_\varepsilon'(\zeta)^2 \to \sigma\delta(\zeta)$ and $\varepsilon|\nabla\zeta|\chi_\varepsilon'(\zeta)^2 \to \sigma\delta_\Sigma$ as $\varepsilon\to 0$. This suggests the following regularization of the excess free energy associated with the surface,

$$\rho f_\varepsilon^{\mathrm{surf}} = \frac{\varepsilon}{|\nabla\zeta|}\nabla\chi_\varepsilon(\zeta)^2 = \varepsilon|\nabla\zeta|(\chi_\varepsilon'(\zeta))^2, \tag{2.15}$$

which agrees with the singular part of (2.5) in the limit $\varepsilon\to 0$. In order to obtain the expression for the corresponding excess stress tensor $\boldsymbol{P}_\varepsilon^{\mathrm{surf}}$, we calculate the rate of change of the surface energy,

$$F_\varepsilon^{\mathrm{surf}} = \int_\Omega \rho f_\varepsilon^{\mathrm{surf}}\,\mathrm{d}x, \tag{2.16}$$

where $\Omega=\Omega_1\cup\Omega_2$. Since the interface is advected with the flow and the following identities hold:

$$\begin{aligned}(\nabla\zeta)^{\cdot} &= -\nabla\boldsymbol{v}\cdot\nabla\zeta,\\ \frac{\mathrm{d}}{\mathrm{d}t}\left(\int_\Omega |\nabla\zeta|\,\mathrm{d}^3x\right) &= \int_\Omega |\nabla\zeta|[(\mathbf{1}-\boldsymbol{n}\otimes\boldsymbol{n}):\nabla\boldsymbol{v}]\,\mathrm{d}^3x,\end{aligned}$$

we get

$$\frac{\mathrm{d}}{\mathrm{d}t}(F_\varepsilon^{\mathrm{surf}}) = \int_\Omega \varepsilon|\nabla\zeta|\chi_\varepsilon'(\zeta)^2(\mathbf{1}-\boldsymbol{n}\otimes\boldsymbol{n}):\nabla\boldsymbol{v}\,\mathrm{d}^3x, \tag{2.17}$$

where $\boldsymbol{a}:\boldsymbol{b}=a_{ij}b_{ij}$. Given that the time derivative of the energy equals the rate of work done on the surface, it is straightforward to conclude that

$$\boldsymbol{P}_\varepsilon^{\mathrm{surf}} = \varepsilon|\nabla\zeta|\chi_\varepsilon'(\zeta)^2(\mathbf{1}-\boldsymbol{n}\otimes\boldsymbol{n}), \tag{2.18}$$

which agrees with the singular part of (2.6) in the limit $\varepsilon \to 0$. By direct calculation, the divergence of the stress tensor in (2.18) is

$$\operatorname{div} \boldsymbol{P}_\varepsilon^{\mathrm{surf}} = 2\varepsilon |\nabla\zeta| \chi_\chi'(\zeta)^2 \kappa(\zeta) \boldsymbol{n}. \tag{2.19}$$

Notice that $\boldsymbol{n}$ (normal) and κ (curvature) are interpreted here as parameters corresponding to the appropriate contour line $\zeta(\boldsymbol{x}, t) = \text{const}$. The term (2.19) is responsible for the pressure jump across the interface in the limit $\varepsilon \to 0$ (Laplace formula (2.13)). This term was first introduced by Brackbill *et al.* (1994). To our knowledge, the above derivation and the expression for the excess stress (2.18) are new.

Let us now show that the regularized stress tensor (2.18) is sensitive to the choice of smoothing, particularly when the interface curvature is large. Consider, for simplicity, a spherically symmetric solution of the level set equations describing a spherical droplet of fluid 1 inside an infinite domain occupied by the fluid 2. In statics, the following equilibrium equation holds:

$$\operatorname{div}(-p\boldsymbol{1} + \varepsilon |\nabla\zeta| \chi_\varepsilon'(\zeta)^2 (\boldsymbol{1} - \boldsymbol{n} \otimes \boldsymbol{n})) = 0, \tag{2.20}$$

or, equivalently,

$$p_r + \frac{2\varepsilon}{r} \chi_\varepsilon'(\zeta)^2 \zeta_r = 0. \tag{2.21}$$

Since $\chi_\varepsilon(\zeta)$ and $\zeta(r)$ are given functions, we integrate (2.20) to get the resulting jump in pressure,

$$p_0 = p_\infty + 2\varepsilon \int_0^\infty \frac{1}{r} \chi_\varepsilon'(\zeta)^2 \zeta_r \, \mathrm{d}r, \tag{2.22}$$

where $p_0 = p(0)$ and $p_\infty = p(\infty)$. Assume for determinacy that the level set function is the distance function from a sphere with radius R_0 centred at the origin, i.e. $\zeta(r) = r - R_0$. Let $\chi_\varepsilon(\zeta)$ be the simple piecewise linear approximation of the Heaviside function,

$$\chi_\varepsilon'(\zeta) = \begin{cases} 0, & \zeta \leqslant 0, \\ \sigma/\varepsilon, & \varepsilon/\sigma > \zeta > 0, \\ 0, & \zeta \geqslant \varepsilon/\sigma. \end{cases} \tag{2.23}$$

Then, if the radius is large ($R \gg \varepsilon/\sigma$), we obtain

$$p_0 - p_\infty = \frac{2\sigma}{R_0} + O\left(\frac{\varepsilon}{\sigma R_0}\right), \tag{2.24}$$

which yields the Laplace formula (2.13) in the limit. However, if the radius is small ($0 < R_0 < \varepsilon/\sigma$), we obtain

$$p_0 - p_\infty = 2\frac{\sigma^2}{\varepsilon} \ln\left[1 + \frac{\varepsilon}{\sigma R_0}\right], \tag{2.25}$$

which, for fixed ε, diverges logarithmically as $R_0 \to 0$. This is to be compared with the $1/R_0$ divergence in the classical case (2.13). A different behaviour is obtained by taking

$$\varepsilon \chi_\varepsilon'(\zeta)^2 = \begin{cases} \sigma(1 + \cos\pi\zeta)/2\varepsilon, & |\zeta| \leqslant \varepsilon, \\ 0, & |\zeta| > \varepsilon, \end{cases} \tag{2.26}$$

which is the approximation of a delta function originally used by Peskin in the boundary method (Peskin 1977). For large R_0, the formula (2.24) is recovered, however, now there is a finite critical radius $R_0^* = \varepsilon$ such that the pressure jump is finite in the limit $R_0 \to R_0^*$ and is not defined for $R_0 < R_0^*$. These two examples certainly do not cover all the possibilities.

We observe, however, that the field χ_ε, which is trivially advected by the flow in the level set method, can be interpreted as describing the concentration of one of the components of the binary fluid. This suggests that the theory should involve the possibility of mixing of the two fluids and should introduce a realistic concentration field $c(\boldsymbol{x}, t)$, evolving according to a suitable diffusion model coupled to the equations of fluid flow. This idea of a physically motivated level set method constitutes the basis of our partial miscibility regularization.

To be more specific, consider a heterogeneous mixture of two fluids with mass concentrations $c_i = M_i/M$, $i = 1, 2$. Here, M_i are the masses of the components in the representative material volume V. Since $M = M_1 + M_2$, we have $c_1 + c_2 = 1$, and let $c = c_1$. Suppose that the two fluids move with different velocities $\boldsymbol{v}_i$ and have different apparent densities $\tilde{\rho}_i = M_i/V$. Then the equation of mass balance for each component can be written in the form,

$$\frac{\partial \tilde{\rho}_i}{\partial t} + \operatorname{div}(\tilde{\rho}_i \boldsymbol{v}_i) = 0.$$

Introduce the mass-averaged velocity $\rho \boldsymbol{v} = \tilde{\rho}_1 \boldsymbol{v}_1 + \tilde{\rho}_2 \boldsymbol{v}_2$, where $\rho = \tilde{\rho}_1 + \tilde{\rho}_2 = M/V$ is the total density. Then

$$\frac{\partial \rho}{\partial t} + \operatorname{div}(\rho \boldsymbol{v}) = 0.$$

The actual mass densities $\rho_i = M_i/V_i$ are related to apparent mass densities $\tilde{\rho}_i$ through $\tilde{\rho}_i = \gamma_i \rho_i$, where $\gamma_i = V_i/V$ are the volumetric fractions. If the excess volume of mixing is equal to zero (for instance, if γ_1 is identified with $V^{-1} \int_V \chi \, \mathrm{d}x$), we obtain an approximation of simple mixture (e.g. Joseph & Rennardy 1993), in particular $\rho^{-1}(c) = \rho_1^{-1} + \rho_2^{-1}(1 - c)$. We remark that the above model of the mixing layer is different from the more traditional models of homogeneous mixtures (see Atkin & Crane (1976) and Bedford & Drumheller (1983) for comprehensive reviews).

Now we make assumptions about the energy of mixing. A fundamental fact of the chemical thermodynamics of fluid mixtures is that even at low temperatures, there is a limited miscibility between the so-called immiscible fluid components. This partial miscibility is characterized by equilibrium concentrations $c_1 \approx 0$ (of the second component in fluid 1) and $c_2 \approx 1$ (of the second component in fluid 2). As the temperature increases, the two equilibrium concentrations approach each other and eventually coincide so that the miscibility gap $c_2 - c_1$ closes at a critical temperature. Above the critical temperature, the system exhibits a continuous sequence of molecular mixtures (solutions), for all $c \in [0, 1]$, and the fluids are considered to be completely miscible. Below the critical temperature, the equilibrium concentrations can be obtained by the standard methods of equilibrium thermodynamics. The particular model of mixing at a given temperature is formulated in terms of the specific free energy $f = f(c)$ which is assumed to be convex if fluids are miscible and nonconvex if fluids are only partially miscible. The method of determining equilibrium concentrations is based on the following common tangent construction:

$$\left.\frac{\mathrm{d}f}{\mathrm{d}c}\right|_{c_1} = \left.\frac{\mathrm{d}f}{\mathrm{d}c}\right|_{c_2}, \qquad \left.\left(f - c\frac{\mathrm{d}f}{\mathrm{d}c}\right)\right|_{c_1} = \left.\left(f - c\frac{\mathrm{d}f}{\mathrm{d}c}\right)\right|_{c_2}, \tag{2.27}$$

which is due to Gibbs (1875*a*,*b*). Further details concerning the thermodynamics of partially miscible fluids can be found in Landau & Lifshitz (1958).

In order to describe a continuous time-dependent concentration profile, we need an additional dynamical equation for $c(\boldsymbol{x}, t)$ that is compatible with the equilibrium conditions (2.27). We postulate that the relative motion of the fluids can be described by a diffusional model. Then

$$\rho\dot{c} = \mathrm{div}(\boldsymbol{J}), \tag{2.28}$$

where the classical assumption for diffusional flux $\boldsymbol{J}$ is Fick's law,

$$\boldsymbol{J} = \nu\nabla\frac{\mathrm{d}f}{\mathrm{d}c}. \tag{2.29}$$

The convective derivative in (2.28) uses the mass-averaged velocity (introduced above) and ρ is the total density of the mixture. The diffusion equation (2.28) can now be written as

$$\rho\dot{c} = \mathrm{div}(D\nabla c), \qquad D = \nu\mathrm{d}^2 f/\mathrm{d}c^2. \tag{2.30}$$

If $f(c)$ is non-convex, there is a domain of concentrations where the mixture is unstable ($\mathrm{d}^2 f/\mathrm{d}c^2 < 0$) and the diffusivity is negative ($D(c) < 0$). This domain is known as the spinodal region and, inside this domain, the initial-value problem for (2.30) is ill-posed (backwards diffusion). To regularize the problem, Cahn & Hilliard (1958) added concentration gradients to the expression for the free energy (weak non-locality)

$$f(c, \nabla c) = f_0(c) + \tfrac{1}{2}\varepsilon|\nabla c|^2, \tag{2.31}$$

and replaced the derivative $\mathrm{d}f/\mathrm{d}c$ in (2.29) by the variational derivative

$$\frac{\delta f}{\delta c} = \frac{\partial f}{\partial c} - \mathrm{div}\left(\frac{\partial f}{\partial \nabla c}\right). \tag{2.32}$$

Then, (2.28) takes the form

$$\rho\dot{c} = \mathrm{div}\left(\nu\nabla\left(\frac{\mathrm{d}f_0}{\mathrm{d}c} - \varepsilon\nabla^2 c\right)\right), \tag{2.33}$$

which is known as the Cahn–Hilliard (CH) equation. In the case of planar equilibrium, this model is compatible with the conditions (2.27). The CH equation was originally derived to describe the linear regime of spinodal decomposition, or the near-critical behaviour of mixtures, when the concentration gradients are small. Equation (2.31), however, is generally considered to be valid throughout the nonlinear regime of fluid separation even when the concentration gradients become large (see, for instance, Kikuchi & Cahn 1962; Elliot 1989).

3. Governing equations

In this section, we derive a system of equations for two-component (binary) fluids in which the components are immiscible and Cahn–Hilliard diffusion is coupled with inertial fluid motion. Suppose that the specific free energy depends, in addition to density ρ and temperature T, on both the concentration of the constituent c and its spatial gradient ∇c, i.e.

$$f = f(\rho, T, c, \nabla c). \tag{3.1}$$

In order to emphasize the role of reactive coupling, and the particular kind of elasticity which the dependence of the energy on gradients brings to the fluid flow, we begin with an analysis of the conservative variant of the model. We assume that the motion is isothermal and that all dissipative processes are infinitely slow on the time-scale of the hydrodynamic problem. Later, we focus on dissipative mechanisms such as diffusion, viscosity and heat conductivity.

For dissipation free flow, the system of governing equations can be obtained from a variational principle where the Lagrangian takes the classical form

$$L = \int_{t_1}^{t_2} \int_{\Omega} \rho(\tfrac{1}{2}|\boldsymbol{v}|^2 - f)\,\mathrm{d}^3x\,\mathrm{d}t. \tag{3.2}$$

Here, $\frac{1}{2}|\boldsymbol{v}|^2$ is the kinetic energy per unit mass and $f(\rho, c, \nabla c)$ is the specific Helmholtz free energy at a given temperature. The five unknown fields are the fluid velocity $\boldsymbol{v}(\boldsymbol{x}, t)$, the mass density $\rho(\boldsymbol{x}, t)$, and the concentration $c(\boldsymbol{x}, t)$. The constraints on the variations of the independent variables are conveniently prescribed in terms of Lagrangian variables.

Let the coordinates $\boldsymbol{\xi}$ label the material particles in the initial configuration and consider a motion of the fluid in the form $\boldsymbol{x} = \boldsymbol{x}(\boldsymbol{\xi}, t)$, where $\boldsymbol{x}$ is the current position of the material particle and $\boldsymbol{x}(\boldsymbol{\xi}, 0) = \boldsymbol{\xi}$. Then, the velocity is given by

$$\boldsymbol{v}(\boldsymbol{\xi}, t) = \dot{\boldsymbol{x}}(\boldsymbol{\xi}, t),$$

where the dot now denotes the partial time derivative at constant $\boldsymbol{\xi}$. The density is given by

$$\rho(\boldsymbol{\xi}, t) = \frac{\rho_0(\boldsymbol{\xi})}{\det|\mathrm{d}\boldsymbol{x}/\mathrm{d}\boldsymbol{\xi}|}, \tag{3.3}$$

where $\rho_0(\boldsymbol{\xi})$ is a given function. In the absence of chemical diffusion, the concentration is advected by the flow, which means

$$c(\boldsymbol{x}, t) = c_0(\boldsymbol{\xi}). \tag{3.4}$$

Now, consider a class of competitors of the fluid flow $\boldsymbol{x} = \boldsymbol{x}(\boldsymbol{\xi}, t, \varepsilon)$. In order to satisfy condition (3.4), we simultaneously vary the concentration field and let $c = c(\boldsymbol{x}, t, \varepsilon)$. Introduce $\delta = \mathrm{d}/\mathrm{d}\varepsilon|_{\varepsilon=0}$ and calculate the first variation of the Lagrangian (3.2). This yields

$$\begin{aligned} \delta L = &-\int_{t_1}^{t_2} \int_{\Omega} ((\rho\dot{\boldsymbol{v}} - \operatorname{div}\boldsymbol{P})\cdot\delta\boldsymbol{x} + \mu\rho\delta c)\,\mathrm{d}^3x\,\mathrm{d}t \\ &- \int_{t_1}^{t^2} \int_{\partial\Omega} (\boldsymbol{P}\boldsymbol{n}\cdot\delta\boldsymbol{x} + \boldsymbol{t}\cdot\boldsymbol{n}\delta c)\,\mathrm{d}S\,\mathrm{d}t + \int_{\Omega} (\rho\boldsymbol{v}\cdot\delta\boldsymbol{x})\mathrm{d}^3x\Big|_{t_1}^{t_2}, \end{aligned} \tag{3.5}$$

where we have used the divergence theorem and the commutation relations responsible for the non-trivial coupling between $\boldsymbol{x}$ and c, i.e.

$$\delta\nabla c - \nabla\delta c = -(\nabla\delta\boldsymbol{x})\nabla c.$$

In equation (3.5), the non-hydrostatic Cauchy stress tensor $\boldsymbol{P}$ is defined by

$$\boldsymbol{P} = -\rho^2 \frac{\partial f}{\partial \rho}\boldsymbol{1} - \rho \nabla c \otimes \frac{\partial f}{\partial \nabla c}. \tag{3.6}$$

The second term in $\boldsymbol{P}$ is the extra reactive stress associated with the presence of concentration gradients (Ericksen's stress (e.g. Ericksen 1991)). The vector $\boldsymbol{t}$ is defined by

$$\boldsymbol{t} = \rho \frac{\partial f}{\partial \nabla c} \tag{3.7}$$

and is a generalized surface force associated with the variation of the concentration on the boundary. The generalized chemical potential μ is defined by

$$\mu = \frac{\partial f}{\partial c} - \frac{1}{\rho}\operatorname{div}\left(\rho \frac{\partial f}{\partial \nabla c}\right). \tag{3.8}$$

We now fix the boundary and the initial displacements and use the constraint $\delta c = 0$. Then, from the condition $\delta L = 0$, we obtain the linear momentum equation,

$$\rho \dot{\boldsymbol{v}} - \operatorname{div}\boldsymbol{P} = 0. \tag{3.9}$$

The balance equations of the mass and the constituent follow from the constraints (3.3) and (3.4) and are given by

$$\dot{\rho} + \rho \operatorname{div}\boldsymbol{v} = 0, \tag{3.10}$$

$$\rho \dot{c} = 0. \tag{3.11}$$

Equations (3.9)–(3.11) form a closed system. The velocity and concentration fields are coupled through the stress tensor (3.6) and through the convective component of the time derivative in (3.11). Because of the assumption (3.4), neither the chemical potential μ nor the generalized force $\boldsymbol{t}$ is manifestly present in (3.9)–(3.11). Both μ and $\boldsymbol{t}$, however, will play an important role in the diffusive part of the model.

Before we add the dissipative terms to the main system of equations, we discuss some important properties of (3.9). Although the stress tensor $\boldsymbol{P}$ is non-hydrostatic, it has a special structure. A direct calculation yields

$$\operatorname{div}\boldsymbol{P} = -\rho(\nabla g - \mu \nabla c), \tag{3.12}$$

where

$$g(\rho, c, \nabla c) = f + \rho \frac{\partial f}{\partial \rho} \tag{3.13}$$

is the specific Gibbs free energy. The identity (3.12) was obtained in Roshin & Truskinovsky (1989) for the special case $\mu = 0$, but for a more general energy function depending on the gradients of arbitrary order. From (3.9) and (3.12), the following expression for the particle acceleration is obtained:

$$\dot{\boldsymbol{v}} = -(\nabla g - \mu \nabla c). \tag{3.14}$$

This formula suggests a generalization of the classical Clebsch representation (Lamb 1945). Let us introduce three auxiliary functions $\Psi(\boldsymbol{x}, t)$, $\alpha(\boldsymbol{x}, t)$, $\beta(\boldsymbol{x}, t)$ which satisfy

$$\dot{\Psi} = \mu, \quad \dot{\alpha} = 0, \quad \dot{\beta} = 0. \tag{3.15}$$

Then, the fluid velocity can be expressed as

$$\boldsymbol{v} = \nabla\varphi + \Psi\nabla c + \alpha\nabla\beta, \tag{3.16}$$

where the potential $\varphi(\boldsymbol{x}, t)$ satisfies the generalized Cauchy–Lagrange integral,

$$\dot{\varphi} = \tfrac{1}{2}\boldsymbol{v}^2 - g. \tag{3.17}$$

To motivate the choices of the Clebsch potentials $\Psi(\boldsymbol{x}, t)$, $\alpha(\boldsymbol{x}, t)$, $\beta(\boldsymbol{x}, t)$, we present here an alternative (Eulerian) variational derivation of the main system of equations.

Consider the original functional L from (3.2) defined in Eulerian coordinates. The independent fields (velocity, density and concentration) are now functions of $\boldsymbol{x}$ and t. We introduce the following class of variations: $\boldsymbol{v} = \boldsymbol{v}(\boldsymbol{x}, t, \varepsilon)$, $\rho = \rho(\boldsymbol{x}, t, \varepsilon)$ and $c = c(\boldsymbol{x}, t, \varepsilon)$. The constraints (3.10) and (3.11) can be added to the functional L with Lagrangian multipliers. As is well known, it is necessary to add an additional constraint in the form $\dot{\beta} = 0$, where $\beta(\boldsymbol{x}, t)$ is an arbitrary function (e.g. Davydov 1949; Salmon 1988). The Lagrangian then takes the form

$$\bar{L} = \int_{t_1}^{t_2} \int_{\Omega} \rho(\tfrac{1}{2}|\boldsymbol{v}|^2 - f(\rho, c, \nabla c) - \Psi\dot{c} - \alpha\dot{\beta}) + \varphi(\dot{\rho} + \rho \operatorname{div} \boldsymbol{v}) \, \mathrm{d}^3x \, \mathrm{d}t,$$

where $\varphi(\boldsymbol{x}, t)$, $\Psi(\boldsymbol{x}, t)$, $\alpha(\boldsymbol{x}, t)$ are Lagrange multipliers. We assume that the initial and boundary conditions are prescribed in such a way that no boundary terms arise when we vary the functional $\bar{L}$. Then, a straightforward calculation shows

$$\begin{aligned} \delta\bar{L} = \int_{t_1}^{t_2} \int_{\Omega} \bigg[& \rho\delta\boldsymbol{v}(\boldsymbol{v} - \nabla\varphi - \Psi\nabla c - \alpha\nabla\beta) + \delta\rho\left(\tfrac{1}{2}\boldsymbol{v}^2 - f - \rho\frac{\partial f}{\partial\rho} - \dot{\varphi} - \Psi\dot{c} - \alpha\dot{\beta}\right) \\ & + \delta c(\Psi(\dot{\rho} + \rho \operatorname{div} \boldsymbol{v}) + \rho(\dot{\Psi} - \mu)) + \delta\varphi(\dot{\rho} + \rho \operatorname{div} \boldsymbol{v}) \\ & - \delta\Psi\rho\dot{c} - \delta\alpha\dot{\beta} + \delta\beta(\rho\dot{\alpha} + \alpha(\dot{\rho} + \rho \operatorname{div} \boldsymbol{v})) \bigg] \, \mathrm{d}^3x \, \mathrm{d}t. \end{aligned}$$

The functional is stationary if, in addition to the constraints (3.3) and (3.4), equations (3.15)–(3.17) are satisfied.

Note that for a single-component fluid, $\nabla c = 0$, and the classical Clebsch representation is recovered. The non-classical term $\Psi\nabla c$ in (3.16) is important as an additional source of fluid vorticity $\boldsymbol{w} = \operatorname{curl}(\boldsymbol{v})$, since

$$\boldsymbol{w} = \nabla\Psi \times \nabla c + \nabla\alpha \times \nabla\beta.$$

Notice also that the chemical potential gradient and the concentration gradient contribute to the generation of vorticity, even in the non-dissipative case, since

$$\dot{\boldsymbol{w}} - \boldsymbol{w} \cdot \nabla\boldsymbol{v} + \boldsymbol{w} \operatorname{div} \boldsymbol{v} = \nabla\mu \times \nabla c.$$

Let us now turn to the dissipative part of the model. We shall derive the governing equations in two steps. Suppose first that the motion is isothermal, the fluids are inviscid, and assume that, in addition to advective transport of the component, there is also chemical diffusion. In order for the mass of each component to be conserved, the following conservation equation must hold:

$$\rho\dot{c} = \operatorname{div} \boldsymbol{J}, \tag{3.18}$$

where $\boldsymbol{J}$ is the diffusional flux vector. To derive constitutive relations for $\boldsymbol{J}$, we use the first and the second laws of thermodynamics as follows.

Consider the integral energy balance (first law of thermodynamics),

$$\frac{\mathrm{d}}{\mathrm{d}t}(E+K) = A + Q, \tag{3.19}$$

where

$$E = \int_{\varOmega} e\rho \,\mathrm{d}^3x, \quad K = \frac{1}{2}\int_{\varOmega} \rho|\boldsymbol{v}|^2 \,\mathrm{d}^3x, \quad A = \int_{\partial\varOmega} (\boldsymbol{P}\boldsymbol{n}\cdot\boldsymbol{v} + (\boldsymbol{t}\cdot\boldsymbol{n})\dot{c})\,\mathrm{d}S$$

are the internal energy, the kinetic energy and the rate of work done on the surface of the material domain $\varOmega$, respectively. The form of A is suggested by our variational analysis in the conservative case (see equation (3.5)). Finally,

$$Q = \int_{\varOmega} r \,\mathrm{d}^3x$$

is the volume rate of heat supply (radiation). In the above, e is the specific internal energy, $\boldsymbol{P}$ is the stress tensor given in (3.6), $\boldsymbol{t}$ is the generalized force defined in (3.7) and r is the density of heat sources necessary to insure that the temperature is constant. Now, suppose that the balance equations (3.9) and (3.10) hold. Then, the local form of the energy balance equation (3.19) is

$$\rho\dot{e} = \boldsymbol{P} : \nabla\boldsymbol{v} + \operatorname{div}(\boldsymbol{t}\dot{c}) + r. \tag{3.20}$$

Using $e = e(\rho, s, c, \nabla c)$, where s is the specific internal entropy and $T = \partial e/\partial s$ is the temperature, equation (3.20) can be rewritten as the balance of entropy

$$\begin{aligned}\rho T\dot{s} = {}& \left(\boldsymbol{P} + \rho^2\frac{\partial e}{\partial\rho}\boldsymbol{1} + \rho\nabla c \otimes \frac{\partial e}{\partial\nabla c}\right) : \nabla\boldsymbol{v} \\ & + \left(\boldsymbol{t} - \rho\frac{\partial e}{\partial\nabla c}\right)\cdot\nabla\dot{c} - \rho\left[\frac{\partial e}{\partial c} - \frac{1}{\rho}\operatorname{div}(\boldsymbol{t})\right]\dot{c} + r\end{aligned} \tag{3.21}$$

(cf. Gurtin 1989). Note that the partial derivatives of the specific internal energy e in (3.21) are equal to the corresponding partial derivatives of the specific Helmholtz free energy $f = e - Ts$. Using the definitions (3.6)–(3.8), equation (3.21) can be simplified to yield

$$\rho T\dot{s} = -\rho\mu\dot{c} + r. \tag{3.22}$$

According to the second law of thermodynamics, in the form of the Clausius–Duhem inequality, we have

$$\rho\chi \geqslant 0 \quad \text{where} \;\; \rho\chi \equiv \rho\dot{s} + \operatorname{div}\mathfrak{I} - r/T, \tag{3.23}$$

where χ is the internal dissipation and $\mathfrak{I}$ is the entropy flux (see Truesdell & Noll 1965). Now, we specify the constitutive models for $\mathfrak{I}$ and χ, to make (3.22) compatible with (3.23). By analogy to the classical theory of (isothermal) diffusion, we assume that

$$\mathfrak{I} = \mu\boldsymbol{J}/T \tag{3.24\,a}$$

and

$$\boldsymbol{J} = \nu\nabla\mu \quad \text{(generalized Fick's law)}, \tag{3.24\,b}$$

where $\nu \geqslant 0$ is the mobility coefficient (see Landau & Lifshitz 1959). This is in agreement with the inequality in (3.23) since

$$\rho\chi = (\nu/T)|\nabla\mu|^2 \geqslant 0. \tag{3.25}$$

With the definitions (3.24) and (3.8), the constituent balance equation (3.18) becomes

$$\rho\dot{c} = \operatorname{div}\left(\boldsymbol{v}\nabla\left(\frac{\partial f}{\partial c} - \frac{1}{\rho}\operatorname{div}\left(\rho\frac{\partial f}{\partial\nabla c}\right)\right)\right), \tag{3.26}$$

which is a compressible analogue of the CH equation (2.33). Alternatives to (3.24), in the case of non-local free energies, are discussed in Truskinovsky (1993).

We are now in a position to add viscosity and heat conductivity to the model. Following Truskinovsky (1993), we generalize the entropy equation (3.22) by adding the viscous stress tensor $\tilde{\boldsymbol{P}}$ and the heat flux vector $\boldsymbol{q}$. Then,

$$\rho T\dot{s} = -\rho\mu\dot{c} + \tilde{\boldsymbol{P}} : \nabla\boldsymbol{v} - \operatorname{div}\boldsymbol{q} + r. \tag{3.27}$$

We also modify (3.24 *a*) to get

$$\mathfrak{J} = (\boldsymbol{q} + \mu\boldsymbol{J})/T, \tag{3.28}$$

so the rate of entropy production takes the form

$$\rho\chi = \frac{\tilde{\boldsymbol{P}} : \nabla\boldsymbol{v}}{T} - \boldsymbol{q}\frac{(\nabla T)}{T^2} + \boldsymbol{J}\nabla\frac{\mu}{T}. \tag{3.29}$$

We now specify the constitutive models of $\tilde{\boldsymbol{P}}$, $\boldsymbol{q}$ and $\boldsymbol{J}$. The simplest model, based on the linear thermodynamics of non-equilibrium processes, assumes linear relations between $\tilde{\boldsymbol{P}}$, $\boldsymbol{q}$, $\boldsymbol{J}$ and $\nabla\boldsymbol{v}$, ∇T, $\nabla\mu$, i.e.

$$\tilde{\boldsymbol{P}} = \boldsymbol{L}_1[\nabla\boldsymbol{v}, \nabla T, \nabla\mu], \qquad \boldsymbol{q} = \boldsymbol{L}_2[\nabla\boldsymbol{v}, \nabla T, \nabla\mu], \qquad \boldsymbol{J} = \boldsymbol{L}_3[\nabla\boldsymbol{v}, \nabla T, \nabla\mu], \tag{3.30}$$

where the linear operators $\boldsymbol{L}_1$, $\boldsymbol{L}_2$ and $\boldsymbol{L}_3$ are chosen to guarantee the non-negativity of $\rho\chi$. Note that since the presence of concentration gradients creates local anisotropy, the relations in (3.30) may be more complicated then those usually assumed in the classical case of an isotropic single-component fluid. For example, the local anisotropy can introduce coupling between the vector and the tensor fluxes. In the relations (3.30), there may be up to five viscosity coefficients and up to two heat conductivity coefficients; the general expressions are discussed in Roshin & Truskinovsky (1989).

In the remainder of this paper, we restrict our attention to the isothermal model with (i) the Cahn–Hilliard specific free energy,

$$f(\rho, c, \nabla c) = f_0(\rho, c) + \tfrac{1}{2}\varepsilon|\nabla c|^2; \tag{3.31}$$

(ii) the diffusion flux $\boldsymbol{J}$ given by the generalized Fick's law (3.24 *b*); and (iii) the viscous stress tensor $\tilde{\boldsymbol{P}}$ given by the classical isotropic two-parameter formula,

$$\tilde{\boldsymbol{P}} = \eta(\nabla\boldsymbol{v} + \nabla\boldsymbol{v}^{\mathrm{T}}) + \lambda(\nabla\cdot\boldsymbol{v})\boldsymbol{1}. \tag{3.32}$$

Then, from the definition (3.6), we obtain the non-viscous contribution to the stress tensor,

$$\boldsymbol{P} = -p_0\boldsymbol{1} - \varepsilon\rho\nabla c\otimes\nabla c = -(p_0 + \varepsilon\rho|\nabla c|^2)\boldsymbol{1} + \varepsilon\rho|\nabla c|^2\left[\boldsymbol{1} - \frac{\nabla c}{|\nabla c|}\otimes\frac{\nabla c}{|\nabla c|}\right], \tag{3.33}$$

where $p_0(\rho, c) = \rho^2\partial f_0/\partial\rho$. It is instructive to compare the reactive contribution to $\boldsymbol{P}$ with the corresponding formula in (2.18) for the regularized extra surface stresses in the level set theory of § 1, identifying $\boldsymbol{n}$ with $\nabla c/|\nabla c|$ and χ_ε, with c. The identification of the second term in (3.33) with $\boldsymbol{P}_\varepsilon^{\mathrm{surf}}$ in (2.18) is straightforward. However, we note that in (3.33), there is an additional spherical component that is absent in the expression used in the level set method.

We finally collect the equations of motion and write the closed system of equations as

$$\left.\begin{aligned} \dot\rho &= -\rho \operatorname{div} \boldsymbol{v}, \\ \rho\dot{\boldsymbol{v}} &= -\nabla p_0 + \operatorname{div}[\eta(\nabla\boldsymbol{v} + \nabla\boldsymbol{v}^{\mathrm{T}}) - \varepsilon\rho\nabla c \otimes \nabla c] + \nabla[\lambda(\nabla\cdot\boldsymbol{v})], \\ \rho\dot c &= \operatorname{div}[\nu\nabla(\mu_0 - (\varepsilon/\rho)\operatorname{div}(\rho\nabla c))], \end{aligned}\right\} \tag{3.34}$$

where $\mu_0(\rho, c) = \partial f_0/\partial c$. These equations describe the motion of a binary viscous compressible fluid. We refer to (3.34) as the Navier–Stokes–Cahn–Hilliard (NSCH) system. We non-dimensionalize the NSCH system as follows. Suppose for simplicity that the dimensional parameters ν, ε and η are constants and assume that the bulk viscosity is equal to zero, i.e. $\lambda = -\frac{2}{3}\eta$. Let L_* and V_* denote the characteristic scales of length and velocity. Then, introduce the dimensionless independent variables $\bar{\boldsymbol{x}} = \boldsymbol{x}/L_*$, $\bar t = V_* t/L_*$ and the following natural scaling of the dependent variables: $\bar{\boldsymbol{v}} = \boldsymbol{v}/V_*$, $\bar\rho = \rho/\rho_*$, $\bar p = p_0(\rho_*\mu_*)$, $\bar\mu_0 = \mu_0/\mu^*$, where again the subscripts denote characteristic quantities. Omitting the bar notation, the NSCH system can now be rewritten as

$$\left.\begin{aligned} \dot\rho &= -\rho \operatorname{div} \boldsymbol{v}, \\ \rho\dot{\boldsymbol{v}} &= -\frac{1}{M}[\nabla p + C \operatorname{div}(\rho\nabla c \otimes \nabla c)] + \frac{1}{Re}(\nabla\boldsymbol{v} + \tfrac{1}{3}\nabla \operatorname{div}\boldsymbol{v}), \\ \rho\dot c &= \frac{1}{Pe}\nabla\left[\mu_0 - C\frac{1}{\rho}\operatorname{div}(\rho\nabla c)\right], \end{aligned}\right\} \tag{3.35}$$

where $Re = \rho_* V_* L_*/\eta$ is the classical Reynolds number, $Pe = \rho_* V_* L_*/(\nu\mu_*)$ is the diffusional Peclet number, $M = V_*^2/\mu_*$ is an analogue of the Mach number and $C = \varepsilon/(\mu_* L_*^2)$ is a measure of the thickness of the interface (Cahn or capillary number). In addition to the main system of equations, we non-dimensionalize the energy of the finite fluid body

$$E = \int_\Omega (\tfrac{1}{2}\boldsymbol{v}^2 + f_0(\rho, c) + \tfrac{1}{2}\varepsilon|\nabla c|^2)\rho \,\mathrm{d}^3x$$

by rescaling $\bar E = E/(L_*^3\rho_* V_*^2)$ and $\bar f_0 = f_0/\mu_*$. Dropping the bar notation, we obtain

$$E = \int_\Omega \rho\{\tfrac{1}{2}\boldsymbol{v}^2 + (1/M)[f_0(\rho, c) + \tfrac{1}{2}C|\nabla c|^2]\}\,\mathrm{d}^3x. \tag{3.36}$$

We note that the parameters Re and Pe are non-dimensional measures of the dissipation in the model, while the parameter C is a non-dimensional measure of the dispersion. When $Re = \infty$ (ECH system), the only source of dissipation is molecular diffusion and the resulting system represents a non-trivial dissipative extension of the Euler equations which is different from the classical Navier–Stokes system.

4. Quasi-incompressibility

In this section, we develop a model of a binary Cahn–Hilliard fluid in which both constituents are incompressible. We call such a fluid quasi-incompressible and show that quasi-incompressibility and incompressibility differ in several important ways. In particular, the density of a quasi-incompressible isothermal fluid may not be constant and the velocity may not be solenoidal. In the context of a theory for miscible fluids, distinctions between quasi-incompressible and incompressible fluids were recently pointed out by Joseph (1990). Here, we begin with a purely thermodynamic definition of quasi-incompressibility and then turn to the dynamic equations.

In classical equilibrium thermodynamics, one can use, as a thermodynamic potential, either the Helmholtz free energy $f(\rho, T, c)$ or the Gibbs free energy $g(p, T, c)$. The two are related through a Legendre transformation. The equivalency between the two descriptions fails if the Legendre transformation becomes degenerate, which is the case in an incompressible fluid.

We first show that the thermodynamic description in terms of the Helmholtz free energy is degenerate in the case of incompressible fluids. Consider, for simplicity, a single-component fluid. If the fluid is compressible and the formula $p = \rho^2 \partial f/\partial \rho$ can be inverted at a given temperature, we obtain $\rho = \rho(p, T)$. Now consider an incompressible fluid, which we take to mean a fluid whose isothermal compressibility is zero:

$$\rho(p, T) = \hat{\rho}(T). \tag{4.1}$$

As a result, p cannot be found uniquely from its thermodynamic definition. Thus, for an incompressible fluid, the mapping between the p–T- and ρ–T-planes is not one-to-one, and the Helmholtz potential $f(\rho, T)$ is not defined off the line $\rho = \hat{\rho}(T)$.

The thermodynamic description in terms of the Gibbs energy $g(p, T)$, however, is still valid for incompressible fluids and the following relations hold:

$$\rho^{-1} = \frac{\partial g}{\partial p}, \qquad s = -\frac{\partial g}{\partial T}, \qquad \mu = \frac{\partial g}{\partial c}. \tag{4.2}$$

We can also formally define a Helmholtz free energy as a function of p, rather than ρ, by

$$f(p, T) = g(p, T) - p\frac{\partial g}{\partial p}. \tag{4.3}$$

In terms of the Gibbs energy, the condition of incompressibility (4.1) is equivalent to

$$\frac{\partial^2 g}{\partial p^2} = 0, \tag{4.4}$$

which is also a condition of the degeneracy of the Legendre transformation limiting the Gibbs and Helmholtz descriptions.

Now consider a binary fluid and suppress, temporarily, the dependence of the Gibbs free energy upon concentration gradients. Assume that condition (4.4) is satisfied for $\hat{g}(p, c, T)$. In spite of the fact that we use the same condition that we used to define a single-component incompressible fluid, we shall refer to the binary fluids satisfying (4.4) as quasi-incompressible instead of incompressible. This is done in order to emphasize that the mixtures made of incompressible components may be compressible at fixed T due to variations of c.

Condition (4.4) implies that the Gibbs energy is a linear function of pressure, i.e.

$$\hat{g}(p, c, T) = \hat{f}(c, T) + \frac{p}{\hat{\rho}(c, T)}, \tag{4.5}$$

where $\hat{f}$ and $\hat{\rho}$ are constants of integration. From (4.2) and (4.3), we conclude that

$$\rho(p,c,T)=\hat{\rho}(c,T) \quad \text{and} \quad f(p,c,T)=\hat{f}(c,T). \tag{4.6}$$

Next, from (4.2), we obtain

$$\mu(p,c,T)=\hat{\mu}\equiv\frac{\partial\hat{f}}{\partial c}-p\hat{\rho}^{-2}\frac{\partial\hat{\rho}}{\partial c}, \tag{4.7}$$

which shows that in quasi-incompressible fluids, the chemical potential explicitly depends on the (kinematic) pressure. The introduction of concentration gradients does not change this analysis in an essential way.

Let us now derive the system of dynamic equations for the isothermal flow of a quasi-incompressible fluid in the presence of diffusion. First, note that from equation (3.10) one can derive

$$\operatorname{div}\boldsymbol{v}=-\frac{\dot{\rho}}{\rho}=-\hat{\rho}^{-1}\left(\frac{\partial\hat{\rho}}{\partial c}\right)\dot{c}. \tag{4.8}$$

Therefore, $\operatorname{div}\boldsymbol{v}$ may be non-zero in the presence of diffusion; this introduces compressibility effects into the model. We next rewrite equation (3.20) by using

$$e=\hat{e}(p,c,\nabla c,T)\equiv\hat{g}+T\hat{s}-p/\hat{\rho},$$

where $\hat{g}(p,c,\nabla c,T)=\hat{f}(c,\nabla c,T)+p/\hat{\rho}(c,T)$ and $\hat{s}=-\partial\hat{g}/\partial T$. Now, since the pressure is no longer defined by standard thermodynamic formulas, we do not assume particular expressions for the stress tensor $\boldsymbol{P}$ and the generalized surface force $\boldsymbol{t}$, and instead follow a standard approach of continuum mechanics based on the Clausius–Duhem inequality (Truesdell & Noll 1965). This gives

$$\hat{\rho}T\dot{s}=\left(\boldsymbol{P}+\hat{\rho}\nabla c\otimes\frac{\partial\hat{f}}{\partial\nabla c}\right):\nabla\boldsymbol{v}-\hat{\rho}\left[\frac{\partial\hat{f}}{\partial c}-\frac{1}{\hat{\rho}}\operatorname{div}(\boldsymbol{t})\right]\dot{c}+\left[\boldsymbol{t}-\hat{\rho}\frac{\partial\hat{f}}{\partial\nabla c}\right]\cdot\nabla\dot{c}+r. \tag{4.9}$$

Since mass is conserved, (3.10) and (4.8) hold. This means that $\nabla\boldsymbol{v}$ and $\dot{c}$ are not independent. Let $\boldsymbol{D}\boldsymbol{v}=\nabla\boldsymbol{v}-(\frac{1}{3}\operatorname{div}\boldsymbol{v})\boldsymbol{1}$ be the deviatoric part of $\nabla\boldsymbol{v}$ and rewrite (4.9) as

$$\begin{aligned}\hat{\rho}T\dot{s}=&\left(\boldsymbol{P}+\hat{\rho}\nabla c\otimes\frac{\partial\hat{f}}{\partial\nabla c}\right):\boldsymbol{D}\boldsymbol{v}+\left[\boldsymbol{t}-\hat{\rho}\frac{\partial\hat{f}}{\partial\nabla c}\right]\cdot\nabla\dot{c}\\&-\left[\frac{1}{3}\left(\operatorname{tr}\boldsymbol{P}+\hat{\rho}\nabla c\cdot\frac{\partial\hat{f}}{\partial\nabla c}\right)\hat{\rho}^{-1}\frac{\partial\hat{\rho}}{\partial c}+\hat{\rho}\left(\frac{\partial\hat{f}}{\partial c}-\frac{1}{\hat{\rho}}\operatorname{div}(\boldsymbol{t})\right)\right]\dot{c}+r,\end{aligned} \tag{4.10}$$

where we have used (4.8). Now, following the approach of § 3, assume that the first two terms on the right-hand side of (4.10) are non-dissipative. Then, we obtain

$$\boldsymbol{P}+\hat{\rho}\nabla c\otimes\frac{\partial\hat{f}}{\partial\nabla c}=-p\boldsymbol{1} \quad \text{and} \quad \boldsymbol{t}=\hat{\rho}\frac{\partial\hat{f}}{\partial\nabla c}, \tag{4.11}$$

where p is an arbitrary scalar. Now, (4.10) reduces to

$$\rho T\dot{s}=-\hat{\rho}\hat{\mu}\dot{c}+r,$$

where

$$\hat{\mu}=\frac{1}{3}\left(\operatorname{tr}\boldsymbol{P}+\hat{\rho}\nabla c\cdot\frac{\partial\hat{f}}{\partial\nabla c}\right)\frac{1}{\hat{\rho}^2}\frac{\partial\hat{\rho}}{\partial c}+\left[\frac{\partial\hat{f}}{\partial c}-\frac{1}{\hat{\rho}}\operatorname{div}(\boldsymbol{t})\right] \tag{4.12}$$

is the generalized chemical potential. Using (4.11), we rewrite (4.12) as

$$\hat{\mu} = -\frac{p}{\hat{\rho}^2}\frac{\partial\hat{\rho}}{\partial c} + \left[\frac{\partial\hat{f}}{\partial c} - \frac{1}{\hat{\rho}}\operatorname{div}\left(\hat{\rho}\frac{\partial\hat{f}}{\partial\nabla c}\right)\right]. \tag{4.13}$$

Hence, in accordance with (4.7), we recover the same linear dependence of the chemical potential on the kinematic pressure as in the preceding thermodynamic analysis. The rest of the derivation follows the pattern described in § 3.

As a result, we obtain the following system of equations governing the motion of quasi-incompressible fluids:

$$\operatorname{div}\boldsymbol{v} = -\frac{1}{\hat{\rho}}\left(\frac{\partial\hat{\rho}}{\partial c}\right)\dot{c}, \tag{4.14a}$$

$$\hat{\rho}\dot{\boldsymbol{v}} = -\nabla p + \operatorname{div}\left[\eta(\nabla\boldsymbol{v} + \nabla\boldsymbol{v}^{\mathrm{T}}) - \varepsilon\hat{\rho}\nabla c \otimes \frac{\partial\hat{f}}{\partial\nabla c}\right] + \nabla[\lambda(\nabla\cdot\boldsymbol{v})], \tag{4.14b}$$

$$\hat{\rho}\dot{c} = \operatorname{div}\left(\nu\nabla\left(\frac{\partial\hat{f}}{\partial c} - \frac{p}{\hat{\rho}^2}\frac{\partial\hat{\rho}}{\partial c} - \frac{1}{\hat{\rho}}\operatorname{div}\left(\hat{\rho}\frac{\partial\hat{f}}{\partial\nabla c}\right)\right)\right). \tag{4.14c}$$

If we further adopt the model of a simple mixture and assume that

$$\hat{\rho}^{-1}(c) = \rho_1^{-1}c + \rho_2^{-1}(1-c), \tag{4.15}$$

where ρ_1 and ρ_2 are constant densities of the constituents (cf. Joseph 1990), equation (4.14 *a*) can be rewritten as

$$\operatorname{div}(\boldsymbol{v} - \alpha\nu\nabla\hat{\mu}) = 0. \tag{4.16}$$

Here we have used equation (4.14 *c*) and let $\alpha = (\rho_2 - \rho_1)/\rho_2\rho_1$. It follows from (4.16) that the velocity field is solenoidal only if the densities are perfectly matched ($\rho_1 = \rho_2$). We note that in Galdi *et al.* (1991), an equation analogous to (4.16) was derived in the context of a theory for miscible fluids.

To obtain the quasi-incompressible NSCH system, we suppose that the free energy takes the form

$$\hat{f}(c, \nabla c) = \hat{f}_0(c) + \tfrac{1}{2}\varepsilon|\nabla c|^2, \tag{4.17}$$

and non-dimensionalize the variables as in § 3. This yields

$$\operatorname{div}\boldsymbol{v} = -\frac{1}{\hat{\rho}}\left(\frac{\partial\hat{\rho}}{\partial c}\right)\dot{c}, \tag{4.18a}$$

$$\hat{\rho}\dot{\boldsymbol{v}} = -\frac{1}{M}[\nabla p + C\operatorname{div}(\hat{\rho}\nabla c\otimes\nabla c)] + \frac{1}{Re}(\nabla\boldsymbol{v} + \tfrac{1}{3}\nabla\operatorname{div}\boldsymbol{v}), \tag{4.18b}$$

$$\hat{\rho}\dot{c} = \frac{1}{Pe}\nabla^2\hat{\mu}, \tag{4.18c}$$

where

$$\hat{\mu} = \mu_0(c) - \frac{p}{\hat{\rho}^2}\frac{\partial\hat{\rho}}{\partial c} - \frac{C}{\hat{\rho}}\operatorname{div}(\hat{\rho}\nabla c), \tag{4.19}$$

and $\hat{\mu}_0(c) = \mathrm{d}\hat{f}_0/\mathrm{d}c$. The initial conditions are given by $\boldsymbol{v}(\boldsymbol{x},0) = \boldsymbol{v}_0(\boldsymbol{x})$ and $c(\boldsymbol{x},0) = c_0(\boldsymbol{x})$. For the velocity, the usual no-slip ($Re < \infty$) or no-flow ($Re = \infty$) boundary conditions can be posed

$$\boldsymbol{v} = \boldsymbol{u}_\Omega \quad \text{or} \quad \boldsymbol{v}\cdot\boldsymbol{n} = \boldsymbol{u}_\Omega\cdot\boldsymbol{n}$$

on $\partial\Omega$, respectively. For the concentration field, Neumann boundary conditions

$$\nabla c \cdot \boldsymbol{n} \quad \text{and} \quad \nabla\mu \cdot \boldsymbol{n} = h_\mu$$

on $\partial\Omega$ are natural and prescribe the generalized force (conjugate to the variation of the concentration of the component on the surface) and the flux of the component; Dirichlet or mixed conditions could be used as well.

To illustrate the role of compressibility in the dynamics of quasi-incompressible fluids, we now consider an elementary one-dimensional model describing the linear stage of spinodal decomposition; the treatment, in a purely diffusional setting with no fluid motion, is due to Cahn (1961). In the density-matched case, our model reduces to the one considered by Cahn. In this case, the fluid equations decouple from the diffusional problem and the condition (4.18 *a*) prevents the flow of the fluid. In general, however, $\alpha \neq 0$ and diffusion driven flow can occur in quasi-incompressible fluids.

To demonstrate this point, consider an inviscid quasi-incompressible fluid with density given by (4.15). Further, let

$$\boldsymbol{v} = u(x,t)\boldsymbol{e}_1, \quad c = c(x,t) \quad \text{and} \quad p = p(x,t), \tag{4.20}$$

where $\boldsymbol{e}_1$ is the unit vector in the x-direction. Assuming there is no overall bulk motion, equations (4.18) and (4.19) yield

$$u = (\alpha/Pe)\hat{\mu}_x. \tag{4.21}$$

With $\alpha \neq 0$, any fluid motion in this one-dimensional setting is a direct result of quasi-incompressibility; an additional coupling between diffusion and motion in dimensions greater than one, induced by viscosity, is discussed by Koga & Kawasaki (1991) and Gurtin *et al.* (1996) among others. Using (4.20) and (4.21) in the ECH system (4.18), (4.19), we obtain the reduced system:

$$\frac{\alpha^2 M}{Pe}\hat{\rho}\left(\hat{\mu}_{xt} + \frac{\alpha}{Pe}\hat{\mu}_x\hat{\mu}_{xx}\right) = (\hat{\mu}_0(c) - \hat{\mu} - Cc_{xx})_x, \tag{4.22}$$

$$\hat{\rho}\left(c_t + \frac{\alpha}{Pe}\hat{\mu}_x c_x\right) = \frac{1}{Pe}\hat{\mu}_{xx}, \tag{4.23}$$

where $\hat{\rho}(c)^{-1} = \alpha c + \rho_2^{-1}$. Next, we linearize this system around the constant state $c = c_*$, $\hat{\mu} = \hat{\mu}_0(c_*)$ and consider solutions of the form $c = c_* + c'(x,t)$, $\hat{\mu} = \hat{\mu}_0(c_*) + \mu'(x,t)$. The linearized equations for the primed variables are given by

$$Pe\hat{\rho}_* c'_t = \mu'_{xx}, \tag{4.24}$$

$$\mu' = \frac{\partial\mu_0(c_*)}{\partial c}c' - Cc'_{xx} - \frac{\alpha^2 M}{Pe}\hat{\rho}_*\mu'_t, \tag{4.25}$$

where $\hat{\rho}_* = \hat{\rho}(c_*)$. For the solutions proportional to $\exp(\lambda t + \mathrm{i}kx)$, we obtain the dispersion relation

$$C(k^2 - k_{\mathrm{c}}^2)k^2 + Pe\hat{\rho}_*\lambda + \alpha^2 M\hat{\rho}_*^2\lambda^2 = 0, \tag{4.26}$$

where

$$k_{\mathrm{c}}^2 = -C^{-1}\frac{\partial\hat{\mu}_0(c_*)}{\partial c} \tag{4.27}$$

is the critical wave number obtained in Cahn (1961). For $\alpha = 0$, the growth rate is

$$\lambda_{\mathrm{c}} = \frac{C}{\hat{\rho}_* Pe} k^2 (k_{\mathrm{c}}^2 - k^2), \tag{4.28}$$

which can also be found in Cahn (1961).

For $\alpha \neq 0$, there are two branches in the dispersion relation. One branch represents the compressible generalization of (4.28) and is given by

$$\lambda_+ = \frac{1}{2}\left[-\frac{Pe}{\alpha^2 M \hat{\rho}_*} + \sqrt{\frac{Pe^2}{\alpha^4 M^2 \hat{\rho}_*^2} - \frac{4C(k^2 - k_{\mathrm{c}}^2)k^2}{\alpha^2 M \hat{\rho}_*^2}}\right]. \tag{4.29}$$

The other branch,

$$\lambda_- = \frac{1}{2}\left[-\frac{Pe}{\alpha^2 M \hat{\rho}_*} - \sqrt{\frac{Pe^2}{\alpha^4 M^2 \hat{\rho}_*^2} - \frac{4C(k^2 - k_{\mathrm{c}}^2)k^2}{\alpha^2 M \hat{\rho}_*^2}}\right], \tag{4.30}$$

describes 'sonic' waves. For $\alpha \neq 0$ and large k, we have both dispersion ($\mathrm{Im}(\lambda_\pm) \approx k^2$) and dissipation ($\mathrm{Re}(\lambda_\pm) = -Pe/(\alpha^2 M \hat{\rho}_*)$). This is in contrast with the case $\alpha = 0$ where, at large k, $\mathrm{Re}(\lambda_{\mathrm{c}}) \approx -k^4$ and $\mathrm{Im}(\lambda_{\mathrm{c}}) = 0$. Notice that for c_* lying in the spinodal region ($\partial\hat{\mu}_0(c_*)/\partial c < 0$), there is an unstable range of wave numbers $|k| \leqslant k^*$ where $\mathrm{Re}(\lambda_+) > 0$. It is interesting that both k^* and k_{m}^*, the wave number corresponding to the maximum growth rate, are independent of α and are unaffected by compressibility. The maximum growth rate $\lambda_+(k_{\mathrm{m}}^*)$, however, is a decreasing function of α. Note also that $\mathrm{Re}\{\lambda_-(k)\} \leqslant 0$, for all k, and no instability is associated with this branch. We remark that there is a finite k^{**} such that for $|k| \geqslant k^{**}$, the real parts of both growth rates coincide and $\mathrm{Re}\{\lambda_\pm\} = -Pe/(2\alpha^2 M \hat{\rho}_*)$.

The two growth rates are illustrated in figure 1, where we have taken $\mu_0(c) = c(c-1)(c-\frac{1}{2})$, $c_* = \frac{1}{2}$ and assumed the scaling $C = \gamma^2$, $Pe = 1/\gamma$, $M = \gamma$. As we discuss in the next section, this is an appropriate scaling that yields a sharp interface limit with a finite surface tension as $\gamma \to 0$.

Finally, let a_k, b_k and d_k be the Fourier amplitudes of $c'(x,t)$, $\mu'(x,t)$ and $u'(x,t)$, respectively. Then,

$$b_k^\pm = -Pe\hat{\rho}_* \frac{\lambda_\pm(k)}{k^2} a_k^\pm \quad \text{and} \quad d_k^\pm = \alpha\hat{\rho}_* \frac{\lambda_\pm(k)}{\mathrm{i}k} a_k^\pm,$$

which means that for perturbations in the unstable interval $|k| \leqslant k^*$, there is a quarter-period phase shift between the velocity and the concentration, and the flow is directed towards the minima of $c'(x,t)$.

5. Sharp interface limit

In this section (with details in the appendix), we show that when the interfacial thickness is small (compared to the radius of curvature of the interfacial layer and the distance between layers), the appropriately scaled ECH system converges to the classical sharp interface model (with surface tension) described in § 2. For simplicity, we suppose that the fluid is inviscid and quasi-incompressible. To justify the scaling of the non-dimensional parameters, we begin by considering an elementary special solution describing the structure of an isolated planar interface between two immiscible fluids.

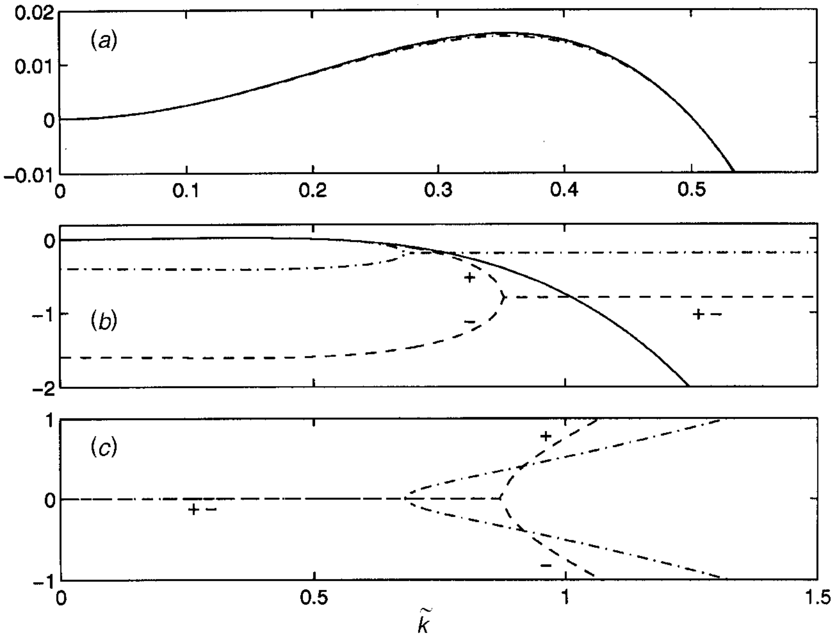

Figure 1. Real and imaginary parts of the growth rates $\tilde{\lambda} = \gamma\hat{\rho}_*\lambda_\pm$ (see (4.29) and (4.30)) as functions of $\tilde{k} = \gamma k$. Close-ups of (*a*) $\mathrm{Re}\{\tilde{\lambda}_\pm\}$, (*b*) $\mathrm{Re}\{\tilde{\lambda}_\pm\}$, (*c*) $\mathrm{Im}\{\tilde{\lambda}_\pm\}$. The +,− indicate the corresponding branches. The parameters are $\gamma = 0.1$ and $\alpha = 0$ (solid curve); $\alpha = 2.5$ (dashed curve); and $\alpha = 5$ (dot-dashed curve).

We assume that the normal to the planar layer is parallel to the z-axis and that the fluid velocity, pressure and concentration are independent of t, x and y. We further suppose there is no fluid velocity in the z-direction. Under these assumptions, the ECH equations (4.18), (4.19) reduce to

$$p_z + C(\hat{\rho}c_z^2)_z = 0, \tag{5.1}$$

$$\left(\frac{\mathrm{d}\hat{f}_0}{\mathrm{d}c} - \frac{p}{\hat{\rho}^2}\frac{\partial\hat{\rho}}{\partial c} - \frac{C}{\hat{\rho}}(\hat{\rho}c_z)_z\right)_{zz} = 0. \tag{5.2}$$

This system is considered on the whole axis with the following boundary conditions:

$$c \to c_\pm \quad \text{and} \quad p \to p_\pm \quad \text{as } z \to \pm\infty. \tag{5.3}$$

We remark that (in the inviscid case) an arbitrary z-dependent motion in the xy-plane can be superimposed. This is a consequence of the fact that in spite of the non-hydrostatic character of the stress tensor, shear motions are decoupled from the concentration problem.

From equation (5.1), we see that for the given concentration field $c(z)$, the pressure $p(z)$ can be obtained from

$$p(z) = p_- - C\hat{\rho}c_z^2. \tag{5.4}$$

To determine the concentration field, we use the Gibbs free energy

$$\hat{g}_0(c) = \hat{f}_0(c) - p_-/\hat{\rho}(c) \tag{5.5}$$

and substitute (5.5) into equation (5.2) to obtain

$$\tfrac{1}{2}Cc_z^2 = \hat{g}_0(c) - \hat{g}_0(c_-) - \mu_-(c - c_-). \tag{5.6}$$

Here, $\mu_- = \mathrm{d}\hat{g}_0/\mathrm{d}c|_{c_-}$. In order for the boundary-value problem (5.3), (5.4) and (5.6) to have a solution, certain constraints on the limiting values (5.3) must be imposed. It is not hard to see that these constraints coincide with the classical thermodynamic conditions of equilibrium:

$$p_+ = p_-, \tag{5.7}$$

$$\left.\frac{\mathrm{d}\hat{g}_0}{\mathrm{d}c}\right|_{c_-} = \left.\frac{\mathrm{d}\hat{g}_0}{\mathrm{d}c}\right|_{c_+}, \tag{5.8}$$

$$\hat{g}_0(c_-) - \left.\frac{\mathrm{d}\hat{g}_0}{\mathrm{d}c}\right|_{c_-} c_- = \hat{g}_0(c_+) - \left.\frac{\mathrm{d}\hat{g}_0}{\mathrm{d}c}\right|_{c_+} c_+. \tag{5.9}$$

As a result, from the four constants $c_\pm$ and $p_\pm$, only one may be chosen independently. The condition (5.7) shows that there is no pressure jump across the interfacial layer which is a consequence of the fact that the interface is flat. In the case of simple mixtures, where the density is given by (4.15), the energies $\hat{g}_0(c)$ and $\hat{f}_0(c)$ differ by a linear function of concentration. Therefore, $\hat{g}_0(c)$ can be replaced by $\hat{f}_0(c)$ in equations (5.6), (5.8) and (5.9) so that (5.8) and (5.9) reduce to the Gibbs conditions (2.28). In the analysis that follows, we only consider simple mixtures.

We now specify the location of the interface z_0 through the balance of the constituent mass

$$\int_{-\infty}^{z_0} (\hat{\rho}c - \rho_- c_-)\,\mathrm{d}z = \int_{z_0}^{+\infty} (\rho_+ c_+ - \hat{\rho}c)\,\mathrm{d}z. \tag{5.10}$$

Given z_0, one can calculate the surface energy associated with the interfacial layer. Let σ be dimensionless excess free energy per unit area, then

$$\sigma = \frac{C}{2M}\int_{-\infty}^{+\infty} \hat{\rho}c_z^2\,\mathrm{d}z + \frac{1}{M}\left[\int_{-\infty}^{z_0} \{\hat{\rho}(c)\hat{f}_0(c) - \rho_-\hat{f}_0(c_-)\}\,\mathrm{d}z + \int_{z_0}^{+\infty} \{\hat{\rho}(c)\hat{f}_0(c) - \rho_+\hat{f}_0(c_+)\}\,\mathrm{d}z\right], \tag{5.11}$$

where we have used formula (3.36). A straightforward calculation using (5.6) and (5.11) yields

$$\sigma = \frac{C}{M}\int_{-\infty}^{+\infty} \hat{\rho}c_z^2\,\mathrm{d}z = \frac{\sqrt{2C}}{M}\int_{c_-}^{c_+} \hat{\rho}(c)\sqrt{\hat{f}_0(c) - \hat{f}_0(c_-) - \left.\frac{\mathrm{d}\hat{f}_0}{\mathrm{d}c}\right|_{c_-}(c - c_-)}\,\mathrm{d}c, \tag{5.12}$$

which shows that σ can be evaluated without reference to the detailed structure of the concentration profile. For example, if the free energy $\hat{f}_0(c)$ is given by

$$\hat{f}_0(c) = \tfrac{1}{4}(c - c_-)^2(c - c_+)^2, \tag{5.13}$$

the coefficient of surface tension is

$$\sigma = \frac{\sqrt{C}}{2M\sqrt{2}}\rho_+\rho_-\frac{(c_+ - c_-)^3}{(\rho_- - \rho_+)^2}\left[\rho_+ + \rho_- + \frac{2\rho_+\rho_-}{\rho_- - \rho_+}\ln\frac{\rho_+}{\rho_-}\right]. \tag{5.14}$$

In this particular case, the concentration distribution $c(z)$ and pressure distribution $p(z)$ can also be found explicitly:

$$c(z) = \tfrac{1}{2}(c_+ + c_-) + \tfrac{1}{2}(c_+ - c_-)\tanh\left[\frac{(c_+ - c_-)(z - z_0)}{2\sqrt{2C}}\right], \tag{5.15}$$

$$p(z) = p_- - \tfrac{1}{32}\hat{\rho}(c)(c_+ - c_-)\,\mathrm{sech}^4\left[\frac{(c_+ - c_-)(z - z_0)}{2\sqrt{2C}}\right]. \tag{5.16}$$

Here, z_0 is the position of the interface from equation (5.10).

Equation (5.12) reveals that both the gradient energy term $\hat{\rho}c_z^2$ and the bulk chemical energy term $\hat{\rho}\hat{f}_0$ contribute equally to the surface energy. This is in contrast with the situation in the level set approach (§ 1), where surface tension arises only from the gradient term (see equation (2.15)).

We now turn to the asymptotic analysis of the ECH equations in the limit when the interfacial layers are thin and isolated. In view of equation (5.15), the sharp interface limit involves taking $C \to 0$. Also, equation (5.12) shows that in order to have a finite surface tension coefficient in this limit, the generalized Mach number must satisfy $M \sim \sqrt{C}$. Therefore, it is natural to introduce a small parameter $\gamma = \sqrt{C}$ as a measure of the thickness of the interface, and to assume the scaling $M = \gamma$. This essentially fixes the coefficient of surface tension. We also take $Pe = 1/\gamma$, which means that diffusion is assumed to be slow. The scaling of M implies that the characteristic velocity $V_* \ll \sqrt{\mu_*}$, while the scaling of Pe is equivalent to the following restriction on the mobility $\nu \ll \rho_* L_*/\sqrt{\mu_*}$. Similar scaling has recently been used by Gurtin *et al*. (1996) and Golovaty (1996) in the framework of model H. We remark that the sharp interface limit can also be obtained by using the assumption of faster diffusion, say $Pe = 1$ (cf. Starovoitov 1994).

Using the above scaling (and $Re = \infty$), we rewrite the ECH system as

$$\operatorname{div}\boldsymbol{v} = -\frac{1}{\hat{\rho}}\left(\frac{\partial\hat{\rho}}{\partial c}\right)\dot{c}, \tag{5.17}$$

$$\hat{\rho}\dot{\boldsymbol{v}} = -(1/\gamma)[\nabla p + \gamma^2\operatorname{div}(\hat{\rho}\nabla c \otimes \nabla c)], \tag{5.18}$$

$$\hat{\rho}\dot{c} = \gamma\nabla\hat{\mu}, \tag{5.19}$$

where

$$\hat{\mu} = \frac{\mathrm{d}\hat{f}_0}{\mathrm{d}c} - \frac{p}{\hat{\rho}^2}\frac{\partial\hat{\rho}}{\partial c} - \frac{\gamma^2}{\hat{\rho}}\operatorname{div}(\hat{\rho}\nabla c). \tag{5.20}$$

We show in the appendix that this system, in the case of an isolated transition layer, is compatible with the sharp interface incompressible Euler model in the limit $\gamma \to 0$.

6. Example of a topological transition

If the curvature of the transition layer is large, e.g. $\kappa = O(1/\sqrt{C})$, then the asymptotic analysis presented in the previous section breaks down. For this type of transition layer, the NSCH system behaves differently from the sharp interface model. For example, in the sharp interface model for inviscid fluids, the Laplace formula says that the pressure diverges at large curvatures, which is typical near a topological transition. In the NSCH model, the effective surface tension varies with curvature , which mollifies this divergence. To demonstrate this effect, we consider a simple example of a topological transition: the annihilation (nucleation) of a spherical droplet of one fluid immersed in an infinite reservoir of another fluid. The simplicity of the geometry allows us to investigate the fine structure of the diffuse interface when the radius of the drop is $O(\sqrt{C})$.

Suppose that there is no fluid motion, and consider stationary solutions of the quasi-incompressible NSCH system (4.18), (4.19) with spherical symmetry. The resulting system of ordinary differential equations is

$$p_r + (C/r^2)(\hat{\rho} r^2 c_r^2)_r = 0, \tag{6.1}$$

$$\left\{ r^2 \left[\frac{\mathrm{d}\hat{f}_0}{\mathrm{d}c} - \frac{p}{\hat{\rho}^2}\frac{\partial \hat{\rho}}{\partial c} - \frac{C}{\hat{\rho} r^2}(\hat{\rho} r^2 c_r)_r \right]_r \right\}_r = 0, \tag{6.2}$$

which is analogous to the system (5.1), (5.2) for the planar interface. The boundary conditions are given by

$$\lim_{r\to\infty} c(r) = c_\infty \quad \text{and} \quad \lim_{r\to\infty} p(r) = p_\infty. \tag{6.3}$$

Symmetry considerations also require that $c_r \to 0$ as $r \to 0$. Contrary to the planar case, the constants c_∞ and p_∞ can be chosen independently as we shall see below. While equations (6.1) and (6.2) always have a trivial homogeneous solution $c(r) = c_\infty$ and $p(r) = p_\infty$, we seek non-trivial solutions in which the concentration is a monotone function of r. By varying c_∞, or by varying the mass of the constituent, we can vary the size of the droplet. The corresponding sequence of equilibrium states may also be interpreted as describing a quasi-steady evolution.

As in the planar case, equations (6.1) and (6.2) can be decoupled. If the densities of the fluids are not matched (i.e. $\mathrm{d}\hat{\rho}/\mathrm{d}c \neq 0$), we obtain an integro-differential equation for the concentration field. In fact, equation (6.1) can be integrated to yield

$$p = p_\infty - C\hat{\rho} c_r^2 + 2C \int_r^\infty \hat{\rho}\frac{c_r^2}{r}\,\mathrm{d}r, \tag{6.4}$$

while equation (6.2) can be transformed to

$$-\tfrac{1}{2}C c_r^2 = \hat{f}_0(c) - [\hat{f}_0(c_\infty) + \mu_\infty(c - c_\infty)] + \left(\frac{p}{\hat{\rho}} - \frac{p_\infty}{\hat{\rho}_\infty}\right), \tag{6.5}$$

where $\mu_\infty = \mathrm{d}\hat{f}_0/\mathrm{d}c(c_\infty)$ and $\hat{\rho}_\infty = \hat{\rho}(c_\infty)$. From equations (6.4) and (6.5), we obtain the following necessary conditions for the existence of a non-trivial solution:

$$p_0 = p_\infty + 2C \int_0^\infty \hat{\rho}\frac{c_r^2}{r}\,\mathrm{d}r, \tag{6.6}$$

$$\hat{f}_0(c_0) - [\hat{f}_0(c_\infty) + \mu_\infty(c_0 - c_\infty)] + \left(\frac{p_0}{\hat{\rho}_0} - \frac{p_\infty}{\hat{\rho}_\infty}\right) = 0, \tag{6.7}$$

where $p_0 = p(0)$, $c_0 = c(0)$ and $\hat{\rho}_0 = \hat{\rho}(c_0)$. These conditions are analogous to conditions (5.7)–(5.9) in the planar case. Since there are only two equations for the four unknowns, c_0, c_∞, p_0 and p_∞, we see that c_∞ and p_∞ can be chosen independently of each other.

In order to compare the diffuse fluid drop with a sharp interface drop, we introduce an effective radius through the mass balance condition (analogous to equation (5.10) defining z_0 in the planar case). For simplicity, we suppose that the density is given by the simple mixture formula (4.15). The effective radius of the diffuse drop, R_0, is implicitly given by the following condition:

$$\int_0^{R_0} [\hat{\rho}(c)c - \hat{\rho}(c_0)c_0] r^2 \,\mathrm{d}r = \int_{R_0}^{\infty} [\hat{\rho}(c_\infty)c_\infty - \hat{\rho}(c)c] r^2 \,\mathrm{d}r. \tag{6.8}$$

Since the drop's surface is diffuse, this choice of an effective radius is obviously not unique. Using this value R_0, we can define the excess surface energy per unit area by the formula

$$\sigma^* = \frac{1}{MR_0^2}\left\{\tfrac{1}{2}C\int_0^\infty \hat{\rho} c_r^2 r^2 \,\mathrm{d}r + \int_0^{R_0} [\hat{\rho}(c)\hat{f}_0(c) - \hat{\rho}(c_0)\hat{f}_0(c_0)] r^2 \,\mathrm{d}r \right. \\ \left. + \int_{R_0}^{\infty} [\hat{\rho}(c)\hat{f}_0(c) - \hat{\rho}(c_\infty)\hat{f}_0(c_\infty)] r^2 \,\mathrm{d}r \right\}, \tag{6.9}$$

which is analogous to (5.11) in the planar interface case. Contrary to the planar case, however, σ^* cannot be evaluated without first computing the full concentration profile $c(r)$. We can simplify (6.9), though, to obtain

$$\sigma^* = \frac{C}{M}\int_0^\infty c_r^2 \left[\frac{r^2}{3R_0^2} + \frac{2R_0}{3r}\right] \hat{\rho} \,\mathrm{d}r. \tag{6.10}$$

An alternative definition for the coefficient of surface tension can be obtained by generalizing the Laplace formula and writing

$$p_0 = p_\infty + 2(\sigma^{**}/R_0)M, \tag{6.11}$$

which defines σ^{**}. Using equation (6.6), we obtain

$$\sigma^{**} = \frac{C}{M}\int_0^\infty c_r^2 \frac{R_0}{r} \hat{\rho} \,\mathrm{d}r. \tag{6.12}$$

We notice that the expressions for both σ^* and σ^{**} depend explicitly on the effective radius of curvature R_0. To determine R_0, we first obtain the concentration profile by solving equations (6.4) and (6.5), and then use equation (6.8) to obtain

$$R_0 = R_0(c_\infty) = \left\{3\int_0^\infty \left[\frac{\hat{\rho}(c)c - \hat{\rho}(c_\infty)c_\infty}{\hat{\rho}(c_0)c_0 - \hat{\rho}(c_\infty)c_\infty}\right] r^2 \,\mathrm{d}r\right\}^{1/3}. \tag{6.13}$$

Following Cahn & Hilliard (1959), we can analyse the behaviour of R_0, σ^* and σ^{**} in certain limiting cases, without computing the concentration and pressure profiles. For example, in the limit when c_∞ approaches the planar equilibrium concentration c_- from above, we get $\lim_{c_\infty \to c_-} c_0 = c_+$ and $\lim_{c_\infty \to c_-} p_0 = p_\infty$, where c_+ is the other equilibrium concentration for the planar interface. One can see that there is no pressure jump across the diffuse interface in this limit. We further obtain $\lim_{c_\infty \to c_-} \sigma^* = \lim_{c_\infty \to c_-} \sigma^{**} = \sigma$, where σ is the surface energy for the planar interface given in equation (5.12). Therefore, the different definitions of surface tension agree in this limit. Also,

$$\lim_{c_\infty \to c_-} (c_\infty - c_-) R_0(c_\infty) = \frac{2\sigma M}{\hat{\rho}_+}\left(\frac{\mathrm{d}^2 \hat{f}_0}{\mathrm{d}c^2}(c_+)\right)^{-1},$$

which shows how the effective radius R_0 diverges in the vicinity of the planar equilibrium concentration.

Another limiting case occurs when $c_\infty = c_\mathrm{s}$; here, c_s is a spinodal point where $\mathrm{d}^2\hat{f}_0/\mathrm{d}^2c$ changes sign. In this limit, the solution of (6.4) and (6.5) converges to the trivial homogeneous state $c(r) = c_\infty$ and $p(r) = p_\infty$. We remark that the energy difference between the non-trivial and the trivial solutions is finite for $c_- < c_\infty < c_\mathrm{s}$ and tends to zero as $c_\infty \to c_\mathrm{s}$.

To illustrate these limits, as well as the behaviour of the solution in the intermediate range of concentrations, we shall first consider the case where the fluids are density matched and equation (6.2) reduces to the radial Cahn–Hilliard equation,

$$C\left(c_{rr} + \frac{2}{r}c_r\right) = \frac{\mathrm{d}}{\mathrm{d}c}(\hat{f}_0(c) - \mu_\infty c). \tag{6.14}$$

This semilinear equation has been studied extensively by many authors (see, for example, Truskinovsky 1983; Dell'Isola *et al.* 1998). Here, we obtain a new explicit solution by considering a piecewise quadratic free energy $\hat{f}_0(c)$. In this special case, the problem reduces to a system of nonlinear algebraic equations.

The simplest smooth piecewise quadratic function, containing a non-trivial spinodal region, consists of three parabolas:

$$\hat{f}_0(c) = \begin{cases} \tfrac{1}{4}c^2, & c \leqslant \tfrac{1}{6}, \\ \tfrac{1}{8}[\tfrac{1}{16} - (c - \tfrac{1}{2})^2], & \tfrac{1}{6} < c < \tfrac{5}{6}, \\ \tfrac{1}{4}(c-1)^2, & c \geqslant \tfrac{5}{6}. \end{cases} \tag{6.15}$$

Using the energy (6.15), it is straightforward to calculate the solution of equation (6.14) analytically. We obtain three linear equations for c corresponding to each of the three parabolas. We then patch the solution together, insuring the continuity of c and c_r. We find that for $c_\infty \in (0, \tfrac{1}{6})$ and $c_\infty \in (\tfrac{5}{6}, 1)$, there is a unique monotone solution $c(r)$. The solutions are parametrized by c_∞ and depend on R_1 and R_2, the coordinates of the points in r where the parabolas are switched.

After a simple calculation, we obtain

$$c(r) = \begin{cases} (B/r)\mathrm{e}^{-r/\surd 2} + c_\infty, & r \geqslant R_1, \\ \tfrac{1}{2} - 2c_\infty - (1/r)[C\cos(\tfrac{1}{2}r) + D\sin(\tfrac{1}{2}r)], & R_2 < r < R_1, \\ 1 + c_\infty + (A/r)(\mathrm{e}^{r/\surd 2} - \mathrm{e}^{-r/\surd 2}), & r \leqslant R_2, \end{cases} \tag{6.16}$$

where, on the right-hand side, the spatial variable is normalized by $\surd C$. In the analysis that follows, we use the normalized variables $r/\surd C$ and $R_i/\surd C$. The coefficients A, B, C and D can be given in terms of R_1 and R_2, which satisfy the following nonlinear system of algebraic equations:

$$-\beta\left(\frac{1}{\surd 2} + \frac{3}{R_1}\right) = \beta\cot\tfrac{1}{2}(R_2 - R_1) + \frac{R_2}{R_1}\csc\tfrac{1}{2}(R_2 - R_1),$$
$$\frac{3}{R_2} - \frac{1}{\surd 2}\coth\frac{R_2}{\surd 2} = \beta\frac{R_1}{R_2}\csc\tfrac{1}{2}(R_2 - R_1) + \cot\tfrac{1}{2}(R_2 - R_1).$$

Here, $\beta = (\tfrac{1}{6} - c_\infty)/(\tfrac{1}{6} + c_\infty)$. We note that there is a critical value $c_\infty = c_\infty^*$ at which $R_2 = 0$. When $R_2 = 0$, the solution is given by

$$c(r) = \begin{cases} (B/r)\mathrm{e}^{-r/\surd 2} + c_\infty, & r \geqslant R_1^*, \\ \tfrac{1}{2} - 2c_\infty - (D/r)\sin(\tfrac{1}{2}r), & 0 \leqslant r < R_1^*, \end{cases} \tag{6.17}$$

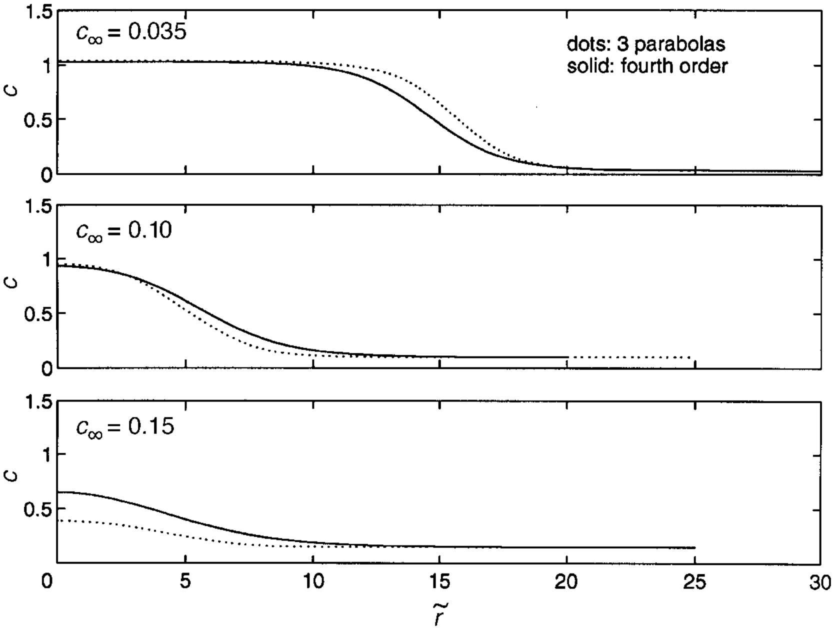

Figure 2. Concentration profiles describing spherical droplets with $c_\infty = 0.035$, 0.10 and 0.15. The dotted curves correspond to the free energy (6.15), while the solid curves correspond the free energy (6.20). The radius is scaled as $\tilde{r} = r/\sqrt{C}$.

where the coefficients B and D can again be expressed in terms of R_1^* and

$$\tan(\tfrac{1}{2}R_1^*) = \frac{R_1^*\sqrt{2}}{R_1^* + 3\sqrt{2}}. \tag{6.18}$$

The critical value c_∞^* is given in terms of R_1^* by

$$c_\infty^* = \frac{R_1^* + 2\sin(\frac{1}{2}R_1^*)}{6(R_1^* - 2\sin(\frac{1}{2}R_1^*))}. \tag{6.19}$$

From (6.18) and (6.19), we obtain $R_1^* \cong 7.764$ and $c_\infty^* \cong 0.117$. For $c_\infty \in (c_\infty^*, \frac{1}{6})$, we also have $R_2 = 0$ and $R_1 = R_1^*$, so the non-trivial monotone solution never reaches the third parabola.

The qualitative change in structure of the solution across $c_\infty = c_\infty^*$ can be viewed as a sign of the beginning of the topological transition. In fact, we can interpret R_2 and R_1 as defining the inner and outer boundaries of the diffuse droplet interface. After the inner boundary R_2 vanishes, the second fluid region disappears and the drop consists entirely of the interfacial region. At larger values of c_∞, the interfacial region also disappears, which marks the completion of the transition. Since no singularities develop, we conclude that the CH model provides a smooth description of this simple topological change. In figure 2, the concentration profiles are shown, as functions of the normalized radius $r/\sqrt{C}$, for three different values of c_∞.

In order to show that the approximation of the energy function by three parabolas is robust, we compare our analytic solution with the results of a direct numerical integration of (6.14) by using the fourth-order polynomial energy

$$\hat{f}_0(c) = \tfrac{1}{4}c^2(c-1)^2, \tag{6.20}$$

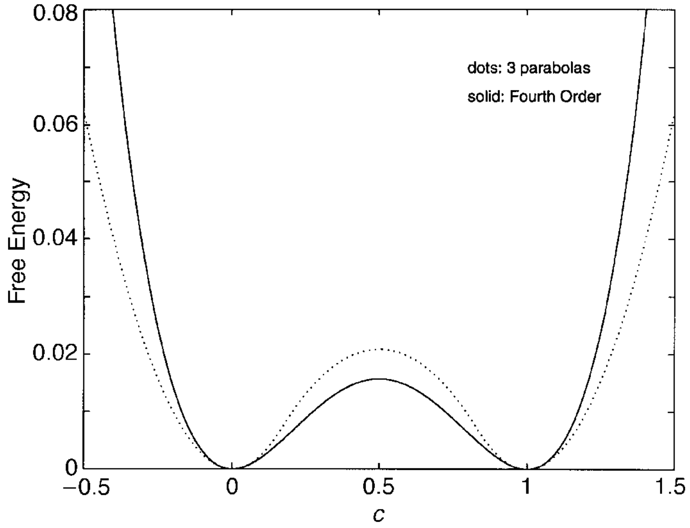

Figure 3. The graphs of the free energies. Solid curve: equation (6.20); dotted curve: equation (6.15).

which is chosen to share the positions and curvatures of the energy wells with (6.15). It is important to remember, however, that the two energies are not 'physically' identical. For example, the spinodal points for the piecewise quadratic free energy are $\frac{1}{6}$ and $\frac{5}{6}$, whereas they are $c_{\mathrm{s}} = \frac{1}{2}(1 \pm 1/\sqrt{3})$ for the fourth-order polynomial (6.20). Moreover, the planar surface energy is also slightly different for the two models: for the free energy given in (6.15), we have

$$\frac{M}{\hat{\rho}\sqrt{C}}\sigma = \frac{3\sqrt{2}}{72} + \sin^{-1}\left(\frac{\sqrt{6}}{3}\right) \cong 0.1385,$$

while for that in (6.20), we have

$$\frac{M}{\hat{\rho}\sqrt{C}}\sigma = \frac{\sqrt{2}}{12} \cong 0.1178.$$

The two free energies are compared in figure 3. The numerical solutions of equation (6.14), with the energy (6.20), are plotted in figure 2 together with the analytic solutions (6.16) and (6.17) of the three-parabola model. A standard first-order accurate shooting method was used to solve (6.14).

In figure 4, we illustrate the behaviour of the normalized effective drop radius $R_0/\sqrt{C}$ as a function of c_∞. The topological transition in the three-parabola model is marked by the vertical dashed line: at this point $c_\infty = c_\infty^*$ and the radius, in the three-parabola model, decreases to a minimum value R_0^*. This value is less than R_1^*. The radius then remains constant for $c_\infty \in [c_\infty^*, \frac{1}{6})$. In the case of the energy (6.20), a similar behaviour is seen until c_∞ approaches the spinodal point $\frac{1}{2}(1 + 1/\sqrt{3})$. The radius reaches a minimum, corresponding to the beginning of the topology transition, and then eventually diverges at the spinodal point (cf. Cahn & Hilliard 1959).

In figure 5, we illustrate the behaviour of the normalized coefficients of surface tension $(M/\hat{\rho}\sqrt{C})\sigma^*$ (dotted curves) and $(M/\hat{\rho}\sqrt{C})\sigma^{**}$ (dashed curves) for the two different free energies, as a function of the normalized effective radius. At large radii, the coefficient of surface tension approaches its value for a flat interface (open circles

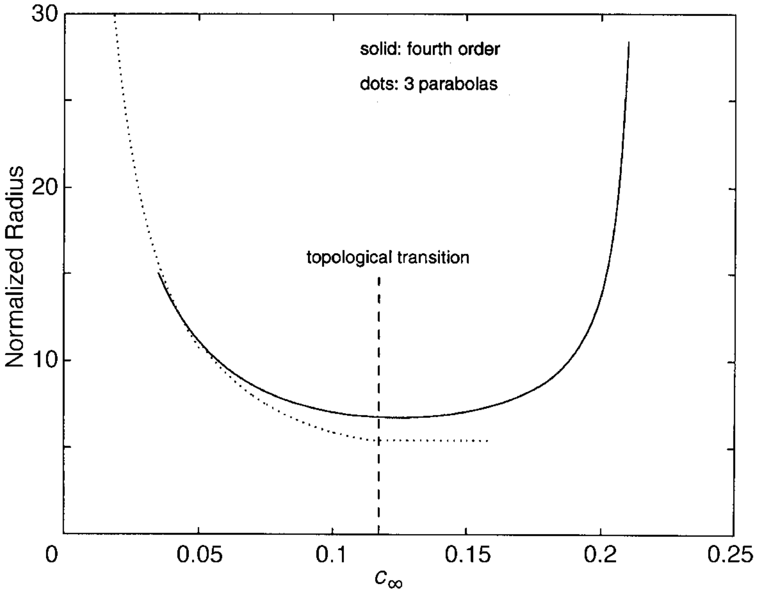

Figure 4. Normalized effective radius of the droplet $\tilde{R}_0 = R_0/\sqrt{C}$ versus c_∞ (dotted curve: the free energy (6.15); solid curve: the free energy (6.20)).

in figure 5). At intermediate radii, the coefficient is a monotone function of curvature. The curvature dependence, however, cannot be extended below a certain radius. In figure 6, the normalized pressure jump $(p_0 - p_\infty)/\hat{\rho}$ is shown as a function of c_∞. We note that the pressure is smooth and finite through the topological change. This is to be contrasted with the classical sharp interface case where the pressure jump diverges when a fluid droplet vanishes.

The introduction of density differences (compressibility) makes the analysis of equations (6.1) and (6.2) considerably more difficult, since the equations become fully nonlinear, even if piecewise quadratic free energies are used. Therefore, we use direct numerical simulations to study this case. We consider the fourth-order free energy given in (6.20) and suppose that the density is given by the simple mixture formula $\hat{\rho}(c)^{-1} = 1 + \theta(c-1)$, where $\rho_+ \equiv \hat{\rho}(1) = 1$ and $\rho_- \equiv \hat{\rho}(0) = 1/(1-\theta)$. Equations (6.1) and (6.2) were solved for different values of θ by using a standard first-order accurate shooting method together with continuation in θ. The pressure jump and effective surface tension for these calculations are presented in figure 7. From this figure, we conclude that, contrary to the dynamic case discussed in § 4, compressibility does not considerably affect the structure of the static spherically symmetric solution.

7. Concluding remarks

The main difference between the conservative sharp interface model (based on the Euler equations) and its dissipative regularizations is that in the conservative model, the topology of the flow is fixed even though the structure of the interface may become highly distorted by the background flow. This is related to the fact that during the process of a topological transition, part of the original information, such as

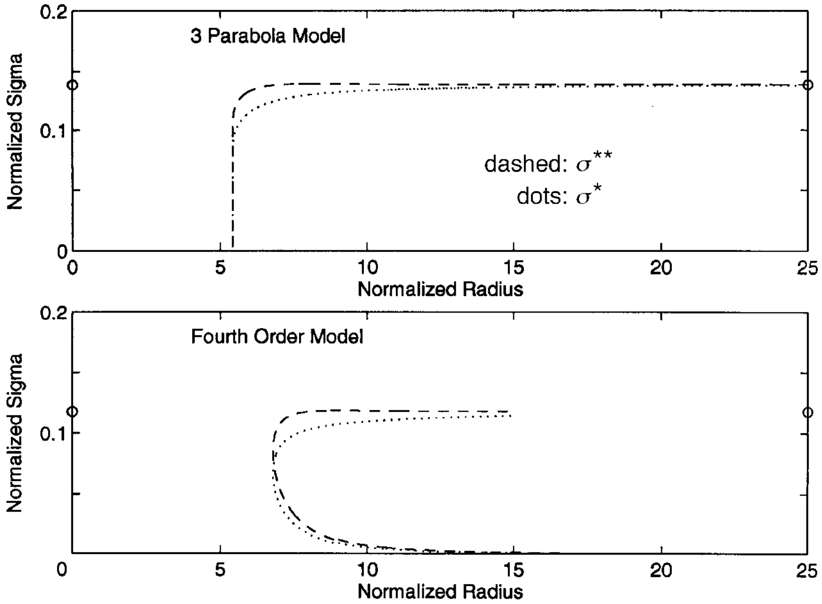

Figure 5. Normalized coefficients of surface tension versus the normalized radius from figure 4. Upper graph: the free energy (6.15); lower graph: the free energy (6.20). Dotted curve: $(M/\hat{\rho}\sqrt{C})\sigma^{*}$ from (6.10). Dashed curve: $(M/\hat{\rho}\sqrt{C})\sigma^{**}$ from (6.12). Open circles: coefficient of surface tension in plane interface case.

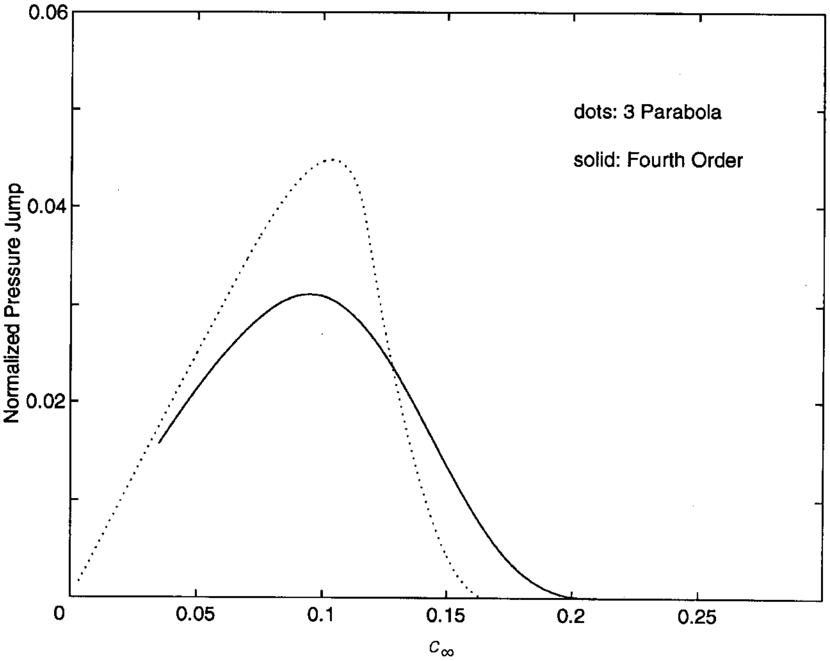

Figure 6. Normalized pressure jump $(p_0 - p_{\infty})/\hat{p}$ versus c_{∞} (dotted curve: the free energy (6.15); solid curve: the free energy (6.20)).

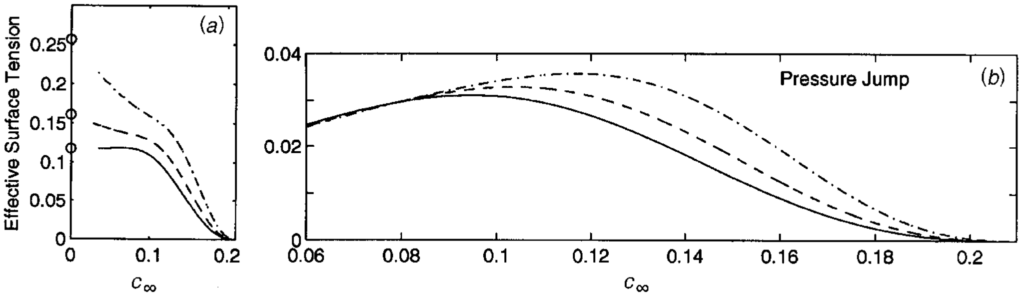

Figure 7. Effects of different densities in the spherically symmetric case. Upper graph: normalized coefficient of surface tension from (6.10) versus c_∞; lower graph: the normalized pressure jump $(p_0 - p_\infty)\hat{p}_\infty$ versus c_∞. Solid curves: $\theta = 0$; dashed curves: $\theta = 0.5$; and dot-dashed curves: $\theta = 0.9$. Open circles in the upper graph: normalized coefficient of surface tension from the plane interface case.

the number of connected components of the flow, may be lost. Topological transitions are associated with a production of entropy (dissipation) and the 'reconnection' conditions must, in particular, prescribe the dissipation associated with the transition.

Often, interface 'surgery' is used to change the topology of sharp interfaces (e.g. Ricca & Berger 1996). One of the main difficulties with this approach is the justification of 'reconnection' conditions (topological 'jump conditions') from the perspective of an augmented regularized theory. In this paper, we have proposed such a regularization of the Euler equations which allows singularity-free topological transitions.

The model takes into account a weak non-locality associated with an internal length scale; this introduces a dimensional surface energy. In the case of near critical binary fluids, with partially miscible components, we anticipate that the model provides a good approximation to the physical problem. One of the main results of this approach is the existence of a small (but finite) size of the zone involved in a topological transition. The transition zone cannot be smaller than the equilibrium (static) thickness of the interface which this theory predicts. However, the non-local theory by itself is non-dissipative and since the non-locality is compatible with classical fluid mechanics integrals, the basic topology of the flow is preserved.

As we mentioned previously, a change of fluid topology cannot take place without dissipative effects and, accordingly, our model takes into account diffusive dissipation which is a natural consequence of using the concentration field. In the limit of infinitely thin and well-separated interfacial layers, we demonstrated that our (appropriately scaled) equations converge to the classical sharp interface model. Since the limiting model is conservative, we conclude that dissipation is localized in the domain where the sharp interface approximation breaks down (say, in the vicinity of a topological transition). Consequently, it may be possible to calculate the associated localized dissipation.

In companion papers (Lowengrub *et al.* 1998*a*, *b*), the ECH model was used to simulate the pinching of density-matched fluid–fluid jets in two dimensions. It was found that in the early stages of the evolution, the dissipation associated with the diffuse layers is negligible and their evolution follows closely that of a sharp interface model (see Hou *et al.* 1994; Lowengrub & Shelley 1997). In the later stages, the fluid flow drives the jet boundaries towards each other and, as the boundaries interact, the energy dissipates rapidly. Although the total energy decreases, the kinetic energy of the fluid increases through the production of vorticity. The calculation captures the topology transition from a two-dimensional jet to a system of fluid droplets.

It was also found that the limiting step in these computations is the resolution of the fluid motion, rather than the structure of the concentration field, and that in order for the concentration boundary layers to be resolved, their thickness needs to be at least several grid lengths. Since the simulations using the ECH model are generically much more expensive than those based on the boundary integral method, it is natural to conclude that the ideal numerical approach should be based on the sharp interface model and then use 'jump conditions' to transit the sharp interface through a topology change.

We view the study of the annihilation of a spherical droplet as a first step in establishing justified 'cut and connect' procedures. In particular, we have shown that the extra energy associated with the nucleus is finite, which effectively fixes the value of dissipation associated with the topological transition. Presently, it is not clear whether such a separation of scales can always be done since the topology change may, in principle, produce fluid fragments that cannot be described within a sharp interface model.

We thank J. Goodman, D. Joseph, P. Leo, G. Lopez, G. McFadden, M. Shelley and Y. Shikhmurzaev for important comments and Elizabeth Lowengrub for proof-reading the manuscript. J.L. acknowledges support from the NSF grant DMS-940310, the Sloan foundation, the McKnight foundation and the Minnesota Supercomputer Institute; L.T. acknowledges support from the NSF grant DMS-9501433 and the Minnesota Supercomputer Institute.

Appendix A. Matched asymptotic expansions

Here we use the method of matched asymptotic expansions to show that the system (5.17)–(5.20) formally converges as $\gamma \to 0$ to the incompressible Euler equations with a sharp interface. In order for our expansions to be valid, the curvature κ of the layer must satisfy $\kappa \ll 1/\gamma$ and the multiple layers must be separated by a distance which is at least $O(1)$. Following the standard approach (see, for example, Pego 1989), we suppose that at time $t = 0$, there is a single smooth transition layer of width $O(\gamma)$. The initial concentration is assumed to be $c(\boldsymbol{x}, 0) = c_\pm + O(\gamma)$ in $\Omega_\pm$, where $c_\pm$ are equilibrium concentrations which satisfy the conditions (5.7)–(5.9) for some $p_\pm$. These initial conditions are consistent with the experiments on the Kelvin–Helmholtz instability performed by Thorpe (1969), where two different fluids were allowed to equilibrate before gravity-induced motion was impulsively started. We further suppose that the most rapid variation in the velocity field for $t > 0$ takes place across the concentration transition layer. This is consistent with assuming that the fluid motion occurs on faster time-scale than the chemical diffusion (our assumption $Pe \gg 1$).

Suppose that in the domains $\Omega_\pm$ (outer region), far from the transition layer, the velocity, concentration and pressure fields can be given in terms of a regular expansion in the small parameter γ, i.e. $A(\boldsymbol{x}, t) = A^{(0)}(\boldsymbol{x}, t) + \gamma A^{(0)}(\boldsymbol{x}, t) + \cdots$, where $A(\boldsymbol{x}, t)$ is a generic variable. Using these expansions in the equations (5.17)–(5.20) and matching powers of γ, we obtain

$$\nabla p^{(0)} = 0$$

at $O(1/\gamma)$, while at $O(1)$, we obtain

$$\operatorname{div} \boldsymbol{v}^{(0)} = 0,$$

$$\hat{\rho}(c^{(0)})(\boldsymbol{v}_t^{(0)} + \boldsymbol{v}^{(0)} \cdot \nabla \boldsymbol{v}^{(0)}) = -\nabla p^{(1)},$$

$$c_t^{(0)} + \boldsymbol{v}^{(0)} \cdot \nabla c^{(0)} = 0,$$

which are the classical Euler equations.

Near the transition layer (inner region), we choose $\phi(\boldsymbol{x}, t)$ to be the signed distance function from a point $\boldsymbol{x}$ to the limiting sharp interfacial surface $\Sigma(t)$ and introduce the stretched normal coordinate $z = \phi(\boldsymbol{x}, t)/\gamma$. Then, $\Sigma(t)$ has unit normal $\boldsymbol{n} = \nabla\phi$, normal velocity $D = -\phi$, and mean curvature $2\kappa = -\nabla^2\phi$. In the inner region, we suppose the following generic expansion holds:

$$A(\boldsymbol{x}, t) = \tilde{A}^{(0)}(z, \hat{\boldsymbol{x}}, t) + \gamma \tilde{A}^{(1)}(z, \hat{\boldsymbol{x}}, t) + \cdots,$$

where $\hat{\boldsymbol{x}}(\boldsymbol{x}, t)$ are two coordinates on the surface $\phi(\boldsymbol{x}, t) = 0$. We use these expansions in equations (5.17)–(5.20), together with the change of variable formulae

$$\nabla = \frac{1}{\gamma}\boldsymbol{n}\partial_z + \nabla_{\hat{\boldsymbol{x}}}, \quad \nabla^2 = \frac{1}{\gamma^2}\partial_{zz} - \frac{2\kappa}{\gamma}\partial_z + \nabla^2_{\hat{\boldsymbol{x}}} \quad \text{and} \quad d_t = -\frac{D}{\gamma}\partial_z + \partial_t.$$

From the normal component of equation (5.18), we obtain at $O(1/\gamma^2)$

$$\tilde{p}_z^{(0)} + (\hat{\rho}(\tilde{c}^{(0)})(\tilde{c}_z^{(0)})^2)_z = 0.$$

At $O(1/\gamma)$, we obtain:

$$\tilde{u}_z^{(0)} = \frac{\hat{\rho}'(\tilde{c}^{(0)})}{\hat{\rho}(\tilde{c}^{(0)})}(\tilde{u}^{(0)} - D)\tilde{c}_z^{(0)}$$

from equation (5.17);

$$\begin{aligned}\hat{\rho}(\tilde{c}^{(0)})(\tilde{u}^{(0)} - D)\tilde{u}_z^{(0)} = -\{&\tilde{p}_z^{(1)} - 2\kappa\hat{\rho}(\tilde{c}^{(0)})(\tilde{c}_z^{(0)})^2 \\ &+ [2\hat{\rho}(\tilde{c}^{(0)})\tilde{c}_z^{(0)}\tilde{c}_z^{(1)} + \hat{\rho}'(\tilde{c}^{(0)})(\tilde{c}_z^{(0)})^2(3\tilde{c}^{(1)} - 2\tilde{c}_z^{(1)})]_z\}\end{aligned}$$

from the normal component of equation (5.18);

$$\begin{aligned}\hat{\rho}(\tilde{c}^{(0)})(\tilde{u}^{(0)} - D)\tilde{\boldsymbol{w}}_z^{(0)} = -[&\nabla_{\hat{\boldsymbol{x}}}\tilde{p}^{(0)} + (\hat{\rho}'(\tilde{c}^{(0)})(\tilde{c}_z^{(0)})^2 \\ &+ \hat{\rho}(\tilde{c}^{(0)})\tilde{c}_{zz}^{(0)})\nabla_{\hat{\boldsymbol{x}}}\tilde{c}^{(0)} + \tfrac{1}{2}\hat{\rho}(\tilde{c}^{(0)})\nabla_{\hat{\boldsymbol{x}}}(\tilde{c}^{(0)})^2]\end{aligned}$$

from the tangential components of equation (5.18); and finally,

$$\hat{\rho}(\tilde{c}^{(0)})(\tilde{u}^{(0)} - D)\tilde{c}_z^{(0)} = \left[\mu_0(\tilde{c}^{(0)}) - \frac{\hat{\rho}'(\tilde{c}^{(0)})}{\hat{\rho}(\tilde{c}^{(0)})}\tilde{p}^{(0)} - \frac{1}{\hat{\rho}(\tilde{c}^{(0)})}(\hat{\rho}(\tilde{c}^{(0)})\tilde{c}_z^{(0)})_z\right]_{zz}$$

from equations (5.19) and (5.20). In the above, $\tilde{u}^{(0)} = \tilde{\boldsymbol{v}}^{(0)} \cdot \boldsymbol{n}$ and $\tilde{\boldsymbol{w}}^{(0)} = \tilde{\boldsymbol{v}}^{(0)} - (\tilde{\boldsymbol{v}}^{(0)} \cdot \boldsymbol{n})\boldsymbol{n}$. We note that if the curvature $\kappa = O(1/\gamma)$, then the local coordinate system near Σ typically becomes singular and the ordering of the above expansions breaks down.

To match the inner and outer expansions, we suppose that the outer expansion holds up to the surface Σ. Then, near Σ, we expand the outer solution in the inner variables and match each power of γ with the limiting values of the inner solution. For example,

$$\lim_{z \to \pm\infty} \tilde{A}^{(0)}(z, \hat{\boldsymbol{x}}, t) = A^{(0)}(\hat{\boldsymbol{x}}, \boldsymbol{t})^{\pm}, \quad \lim_{z \to \pm\infty} \tilde{A}^{(1)}(z, \hat{\boldsymbol{x}}, t) = A^{(1)}(\hat{\boldsymbol{x}}, \boldsymbol{t})^{\pm}$$

$$\lim_{z \to \pm\infty} \tilde{A}_z^{(1)}(z, \hat{\boldsymbol{x}}, t) = \boldsymbol{n} \cdot \nabla A^{(0)}(\hat{\boldsymbol{x}}, \boldsymbol{t})^{\pm},$$

where the ± denotes the limiting values on $\mathit{\Sigma}$ from $\mathit{\Omega}_{\pm}$.

At $O(1/\gamma)$ in the outer expansion, we obtain

$$p^{(0)}(\boldsymbol{x},t)=p_{\pm}=\text{const. in }\mathit{\Omega}_{\pm},$$

although the constant could take different values in each region. From the inner expansion at $O(1/\gamma^2)$, we obtain

$$\tilde{p}^{(0)}(z,\hat{\boldsymbol{x}},t)=p_{-}-\hat{\rho}(\tilde{c}^{(0)})(\tilde{c}_z^{(0)})^2 \quad\text{and}\quad p_{-}=p_{+},$$

which means that (in the leading order) the outer pressure is a global constant.

At $O(1/\gamma)$ in the inner expansion, we obtain

$$\tilde{u}^{(0)}(z,\hat{\boldsymbol{x}},t)=D(\hat{\boldsymbol{x}},t),$$

which, together for the matching condition for velocity, shows that

$$[[\boldsymbol{v}^{(0)}\cdot\boldsymbol{n}]]_{\mathit{\Sigma}}=0 \quad\text{and}\quad \boldsymbol{v}^{(0)}\cdot\boldsymbol{n}=D.$$

Consequently, the interface moves with the fluid at the outer scale. In addition, from the inner expansion, we obtain

$$\tilde{c}^{(0)}(z,\hat{\boldsymbol{x}},t)=C(z+\alpha(\hat{\boldsymbol{x}},t)),$$

where $C(z)$ is the unique planar interface, described in § 5, with $C(0)=\frac{1}{2}(c_{+}+c_{-})$. The function $\alpha(\hat{\boldsymbol{x}},t)$ is an arbitrary translation; this can be set to zero by using a centring condition of the type given in Pego (1989) which links the position of the interfacial surface $\mathit{\Sigma}$ with the inner expansion. Using the matching condition for the concentration and the initial condition for the concentration, we obtain

$$c^{(0)}(\boldsymbol{x},t)=c_{\pm}\quad\text{in }\mathit{\Omega}_{\pm}.$$

Then from the inner expansion, we get

$$\tilde{p}_z^{(1)}=2\kappa\hat{\rho}(\tilde{c}^{(0)})(\tilde{c}_z^{(0)})^2+[2\hat{\rho}(\tilde{c}^{(0)})\tilde{c}_z^{(0)}\tilde{c}_z^{(1)}+\hat{\rho}'(\tilde{c}^{(0)})(\tilde{c}_z^{(0)})^2(3\tilde{c}^{(1)}-2\tilde{c}_z^{(1)})]_z.$$

Using the first-order matching condition for pressure, we conclude that

$$[[p^{(1)}]]_{\mathit{\Sigma}}=2\kappa\int_{-\infty}^{+\infty}\hat{\rho}(C)C_z^2\,\mathrm{d}z,$$

which shows that the jump in the outer pressure $p^{(1)}$ across $\mathit{\Sigma}$ is proportional to the mean curvature of $\mathit{\Sigma}$. We note that the integral in the right-hand side of this formula is exactly the one which appeared in equation (5.12), divided by γ. Finally, we note that equation for the tangential components of linear momentum is trivially satisfied so that the tangential velocity $\tilde{\boldsymbol{w}}^{(0)}$ does not appear at this order. Thus, in the leading order, the jump of the outer tangential velocity (across $\mathit{\Sigma}$) is arbitrary.

These results show that the limiting sharp interface moves with the fluid, the Euler equations hold on each side of the interface and the Laplace condition is satisfied with the surface tension given by equation (5.12). We also notice that the energy (3.36) converges, as $\gamma\to 0$, to the expression

$$E(t)=\tfrac{1}{2}\rho_{+}\int_{\mathit{\Omega}_{+}}|\boldsymbol{v}^{(0)}|^2\,\mathrm{d}^3x+\tfrac{1}{2}\rho_{-}\int_{\mathit{\Omega}_{-}}|\boldsymbol{v}^{(0)}|^2\,\mathrm{d}^3x+\sigma|\mathit{\Sigma}(t)|,$$

which is the energy of the sharp interface model. Here, for simplicity, we assumed $f_0(c_{\pm})=f_0'(c_{\pm})=0$.

References

Aifantis, E. C. & Serrin, J. B. 1983 The mechanical theory of fluid interfaces and Maxwell's rule. *J. Coll. Int. Sci.* **96**, 517–529.

Anderson, D. M. & McFadden, G. B. 1997 A diffuse-interface description of internal waves in near critical fluid. *Phys. Fluids* A **9**, 1870–1879.

Antanovskii, L. 1995 A phase field model of capillarity. *Phys. Fluids* A **7**, 747–753.

Atkin, R. J. & Crane, R. E. 1976 Continuum theories of mixtures: basic theory and historical development. *Q. J. Mech. Appl. Math.* **29**, 209–244.

Bedford, A. & Drumheller, D. S. 1983 Theories of immiscible and structured mixtures. *Int. J. Engng Sci.* **21**, 863–960.

Brackbill, J. U., Kothe, D. B. & Zemach, C. 1994 A continuum method for modelling surface tension. *J. Comp. Phys.* **100**, 335–354.

Cahn, J. W. 1961 On spinodal decomposition. *Acta Metall.* **9**, 795–801.

Cahn, J. W. & Hilliard, J. E. 1958 Free energy of non-uniform system. I. Interfacial free energy. *J. Chem. Phys.* **28**, 258–267.

Cahn, J. W. & Hilliard, J. E. 1959 Free energy of non-uniform system. III. *J. Chem. Phys.* **31**, 688–699.

Chang, Y. C., Hou, T. Y., Merriman, B. & Osher, S. 1996 A level set formulation of Eulerian interface capturing methods for incompressible fluid flows. *J. Comp. Phys.* **124**, 449–464.

Chella, R. & Vinals, J. 1996 Mixing of a two-phase fluid by cavity flow. *Phys. Rev.* E **53**, 3832–3840.

Davis, H. T. & Scriven, L. E. 1982 Stress and structure in fluid interfaces. *Adv. Chem. Phys.* **49**, 57–454.

Davydov, B. 1949 Variational principles and canonical equations for ideal fluid. *Dokl. Akad. Nauk SSSR* **69**, 165–168.

Dell'Isola, F., Gouin, H. & Rotoli, G. 1998 Nucleation of spherical shell-like interfaces by second gradient theory: numerical simulations. *Eur. J. Mech. Fluids* (In the press.)

Eggers, J. 1995 Theory of drop formation. *Phys. Fluids* **7**, 941–953.

Eggers, J. & Dupont, T. F. 1994 Drop formation in a one-dimensional approximation of the Navier–Stokes equations. *J. Fluid Mech.* **262**, 205.

Elliot, C. M. 1989 The Cahn–Hilliard model for the kinetics of phase separation. In *Mathematical models for phase change problems* (ed. J. F. Rodrigues). International Series in Numerical Mathematics, vol. 88, pp. 35. Basel: Birkhäuser.

Ericksen, J. L. 1991 Liquid crystals with variable degree of orientation. *Arch. Ration. Mech. Analysis* **113**, 97–120.

Falk, F. 1992 Cahn–Hilliard theory and irreversible thermodynamics. *J. Non-Equilib. Thermodyn.* **17**, 53–65.

Galdi, P., Joseph, D. D., Preziosi, L. & Rionero, S. 1991 Mathematical problems for miscible, incompressible fluids with Korteweg stresses. *Eur. J. Mech. Fluids* **10**, 253–267.

Gibbs, J. 1875*a* On the equilibrium of heterogeneous substances. *Trans. Connect. Acad.* **111**, 108–248

Gibbs, J. 1875*b* On the equilibrium of heterogeneous substances. *Trans. Connect. Acad.* **111**, 343–524.

Golovaty, D. 1996 On the asymptotic behaviour of the equations describing the motion of an incompressible binary fluid. (Preprint.)

Gurtin, M. 1989 On a non-equilibrium thermodynamics of capillarity and phase. *Q. Appl. Math.* **47**, 129–145.

Gurtin, M. E. & McFadden, G. B. (eds) 1992 *On the evolution of phase boundaries.* IMA Series in Mathematics and its Applications, no. 43. Springer.

Gurtin, M. E., Polignone, D. & Vinals, J. 1996 Two-phase binary fluids and immiscible fluids described by an order parameter. *Math. Models Meth. Appl. Sci.* **6**, 815–831.

Hohenberg, P. C. & Halperin, B. I. 1977 Theory of dynamic critical phenomena. *Rev. Mod. Phys.* **49**, 435–479.

Hou, T. Y., Lowengrub, J. S. & Shelley, M. J. 1994 Removing the stiffness from interfacial flows with surface tension. *J. Comp. Phys.* **114**, 312–338.

Hou, T. Y., Lowengrub, J. S. & Shelley, M. J. 1997 The long-time motion of vortex sheets with surface tension. *Phys. Fluids* A **9**, 1933–1954.

Jacqmin, D. 1998 Contact line dynamics of a diffuse fluid interface. *Phys. Fluids* A. (Submitted.)

Jasnow, D. & Vinals, J. 1996 Coarse-grained description of thermo-capillary flow. *Phys. Fluids* A **8**, 660–669.

Joseph, D. D. 1990 Fluid dynamics of two miscible liquids with diffusion and gradient stresses. *Eur. J. Mech. Fluids* **9**, 565–596.

Joseph, D. D. & Rennardy, Y. Y. 1993 *Fundamentals of two fluid mechanics.* Springer.

Keller, J. B. & Merchant, G. J. 1991 Flexural rigidity of a liquid surface. *J. Stat. Phys.* **63**, 1039–1051.

Keller, J. B. & Miksis, M. 1983 Surface tension driven flows. *SIAM J. Appl. Math.* **43**, 268–277.

Kikuchi, R. & Cahn, J. W. 1962 Theory of domain walls in ordered structures. II. Pair approximations for non-zero temperatures. *J. Phys. Chem. Solids* **23**, 137–151.

Koga, T. E. & Kawasaki, K. 1991 Spinodal decomposition in binary fluids: effects of hydrodynamic interactions. *Phys. Rev.* A **44**(2), R817–R820.

Lamb, H. 1945 *Hydrodynamics.* New York: Dover.

Landau, L. D. & Lifshitz, E. M. 1958 *Statistical physics.* Oxford: Pergamon.

Landau, L. D. & Lifshitz, E. M. 1959 *Fluid mechanics.* Oxford: Pergamon.

Lowengrub, J. S., Shelley, M. J., Truskinovsky, L. & Goodman, J. 1998*a* The break-up of liquid jets in Cahn–Hilliard hydrodynamics. (In preparation.)

Lowengrub, J. S., Goodman, J., Lee, H., Longmire, E., Shelley, M. & Truskinovsky, L. 1998*b* Topological transitions in liquid/liquid interfaces. In *Proc. 1997 Int. Conf. on Free Boundary Problems, Crete.* (In the press.)

Mansour, N. & Lundgren, T. 1990 Satellite formation in capillary jet breakup. *Phys. Fluids* A **2**, 1141–1144.

Myasnikov, V., Roshin, A. & Truskinovsky, L. 1990 Structure of the isothermal shock in weakly non-local relaxing compressible medium. *Dokl. Akad. Nauk SSSR* **311**, 1347–1351.

Osher, S. & Sethian, J. A. 1988 Fronts propagating with curvature-dependent speed: algorithms based on Hamilton–Jacobi formulations. *J. Comp. Phys.* **79**, 12–49.

Pego, R. L. 1989 Front migration in the nonlinear Cahn–Hilliard equation. *Proc. R. Soc. Lond.* A **422**, 261–278.

Peskin, C. 1977 Numerical analysis of blood flow in the heart. *J. Comp. Phys.* **25**, 220–252.

Ricea, R. L. & Berger, M. A. 1996 Topological ideas and fluid mechanics. *Phys. Today* **49**, 28–34.

Roshin, A. & Truskinovsky, L. 1989 Model of weakly non-local relaxing compressible medium. *J. Appl. Math. Mech.* **53**, 904–910.

Salmon, R. 1988 Hamilton fluid mechanics. *A. Rev. Fluid Mech.* **20**, 225–256.

Seppecher, P. 1996 Moving contact lines in the Cahn–Hilliard theory. *Int. J. Engng Sci.* **34**, 977–992.

Sethian, J. A. 1996 *Level set methods.* Cambridge University Press.

Slemrod, M. 1983 Admissibility criteria for propagating phase boundaries in a van der Waals fluid. *Arch. Ration. Mech. Analysis* **81**, 301–315.

Starovoitov, V. N. 1994 Model of the motion of a two-component liquid with allowance of capillary forces. *J. Appl. Mech. Tech. Phys.* **35**, 891–897.

Sussman, M., Smerka, P. & Osher, S. 1994 A level set approach for computing solutions to incompressible two-phase flow. *J. Comp. Phys.* **114**, 146–159.

Thorpe, S. A. 1969 Experiments on the instability of stratified shear flows: immiscible fluids. *J. Fluid Mech.* **39**, 25–48.

Truesdell, C. & Noll, W. 1965 The nonlinear field theories of mechanics. In *The encyclopedia of physics* (ed. S. Flugge), vol. III. Springer.

Truskinovsky, L. 1982 Equilibrium phase boundaries. *Sov. Phys. Dokl.* **27**, 551–553.

Truskinovsky, L. 1983 Critical nuclei in the van der Waals model. *Sov. Phys. Dokl.* **28**, 248–250.

Truskinovsky, L. 1988 Non-equilibrium phase boundaries in the Earth's mantle. *Dokl. Akad. Nauk SSSR* **303**, 1337–1342.

Truskinovsky, L. 1993 Kinks versus shocks. In *Shock induced transitions and phase structures in general media* (ed. R. Fosdick, E. Dunn & M. Slemrod). IMA Series in Mathematics and its Applications, no. 52, pp. 185–229. Springer.

Univerdi, S. O. & Trygvason, G. 1992 A front tracking method for viscous, incompressible multi-fluid flows. *J. Comp. Phys.* **100**, 25–37.

Van der Waals, J. D. 1894 Therinodynamische theorie der kapillaritat unter voraussetzung stetiger dichteanderung. *Z. Phys. Chem.* **13**, 657. (English transl. in *J. Stat. Phys.* **20** (1979).)